Title

Improving Health System Resilience through Continuous Nowcasting of Undetected Public Health Disruption During Floods: A Multi-Country Precision Intelligence Study

Authors

Usman Nazir[1,2] (MEng, PhD)

Manal Shehabi[3,4] (MIA, PhD)

Hamid Mahmood[5] (MSc, PhD)

Elizabeth Stuart[3] (MRes)

Professor Lalith Rajapakse[6] (MSc, PhD)

Rochelle Schneider[7] (MSc, PhD)

Mohammad Kamran[8] (MSc, PhD)

Professor Aluisio Barros[9] (MSc, PhD)

Professor Jere Behrman[10] (PhD)

Neven Fuckar[11] (MSc, PhD)

Khatera Afghan[12] (MSc)

Olivia Vashti Ayim[13] (MSc)

Kerubo Bosire[14] (PhD)

Claudia Cappa[12] (PhD)

Neelima Chopra[15] (MSc, PhD)

Georgina Donati[3, 16] (PhD)

Omnia El-Emrani[3, 17, 18] (MPP)

Leondardo Ferreira[9] (PhD)

Professor Sandy Fredman[19] (PhD)

Liana Ghent[20] (MSc)

Preprint not peer reviewed

This preprint research paper has not been peer reviewed. Electronic copy available at: https://ssrn.com/abstract=7353571

Ghassan Issa[21,22] (MD, Pediatrics Diploma)

Joan Lombardi[23](PhD)

Gabriela Marques[9] (PhD)

Jessica Mendes[11] (PhD)

Lynette Okengo[14] (PhD)

Evelyn Santiago[14] (MA)

Rohini Swaminathan Sampoornam[12] (MBA)

Professor Cesar Victora[9] (PhD)

Victoria Whitford[14] (MSc, MBBS, MRCPsych)

Chemba Raghavan[12] (MSc, PhD)

Professor Myles Allen[13] (DPhil)

Professor Alan Stein [3, 24, 25](MBBS, MRCPsych)

Professor Sara Khalid[1] (MSc, DPhil)

on behalf of the Children and Climate Initiative Consortium.

Affiliations

1. Health Data Sciences, Nuffield Department of Orthopaedics, Rheumatology and Musculoskeletal Sciences (NDORMS), University of Oxford, Oxford, United Kingdom
2. Center for AI Research, Beaconhouse National University, Lahore, Pakistan
3. Blavatnik School of Government, University of Oxford, Oxford, United
4. Institute for New Economic Thinking, University of Oxford, Oxford, United Kingdom
5. UN-SPIDER, United Nations Office for Outer Space Affairs, Beijing, China
6. University of Moratuwa, Sri Lanka
7. European Space Agency, Paris, France
8. Punjab Irrigation Department (PID), Lahore, Pakistan
9. International Center for Equity in Health, Universidade Federal de Pelotas, Pelotas, Brazil
10. School of Arts and Sciences, University of Pennsylvania, Philadelphia, United States of America

Preprint not peer reviewed

This preprint research paper has not been peer reviewed. Electronic copy available at: https://ssrn.com/abstract=7353571

[11] School of Geography and the Environment, University of Oxford, Oxford, United Kingdom
[12] UNICEF, Florence, Italy
[13] Atmospheric, Oceanic and Planetary Physics, University of Oxford, Oxford, United Kingdom
[14] African Early Childhood Network, Nairobi, Kenya
[15] Asia-Pacific Regional Network for Early Childhood (ARNEC)
[16] Departments of Psychiatry and Experimental Psychology, University of Oxford, Oxford, United Kingdom
[17] Ain Shams University, Faculty of Medicine, Cairo, Egypt
[18] Global Climate and Health Alliance,
[19] Faculty of Law, University of Oxford, Oxford, United Kingdom
[20] ISSA International Step by Step Association, Netherlands
[21] Arab Network for Early Childhood (ANECD), Beirut, Lebanon
[22] Arab Resource Collective (ARC), Beirut, Lebanon
[23] Thrive Center for Children, Families and Communities, Georgetown University, Washington, DC, United States of America
[24] School of Public Health, University of Witwatersrand, Johannesburg, South Africa
African Health Research Institute, Durban, Kwazulu Natal, South Africa

Corresponding author

Professor Sara Khalid *B.E., MSc. (Oxon.), DPhil*

Health Data Sciences, Centre for Statistics in Medicine, Botnar Research Centre, NDORMS, University of Oxford, United Kingdom

sara.khalid@ndorms.ox.ac.uk

Preprint not peer reviewed

This preprint research paper has not been peer reviewed. Electronic copy available at: https://ssrn.com/abstract=7353571

Abstract

Background

Climate-exacerbated flooding triggers global public health crises, costing lives, livelihoods, and jeopardising fragile healthcare systems. Despite well-established disaster management frameworks, the timely communication of rapid, locally actionable information remains lacking—leaving vulnerable populations at risk. We developed and operationally validated an open-access monitoring system across six South Asian nations, reporting the public health impact of the 2025 floods and executing live daily nowcasting during the July 2026 monsoon emergency to better understand who is in harms' way, democratise anticipatory disaster intelligence, and support healthcare resilience.

Methods

We engineered a multi-stakeholder co-designed ensemble pipeline for flood-health intelligence by fusing observations from six synthetic aperture radar and optical satellites with hydrological, demographic, agricultural, transportation, and infrastructure datasets. We estimated cumulative exposure for children and adults, alongside functional disruption to healthcare facilities, built-up areas, road networks, and cropland across remote, rural, and urban areas of Pakistan, India, Bangladesh, Bhutan, Nepal, and Sri Lanka. The 2025 analysis was benchmarked against publicly-available official surveillance reports and independent field-validation. The 2026 deployment is ongoing live, externally field-validated against 8 ground-sensor stations along the Indus River system.

Findings

Our analysis revealed a critical gap in current surveillance. In 2025, continuous monitoring identified 257.67 million exposed individuals (29.1% in rural areas) including 89.3 million children under 18 (34.6%). A five-fold increase (72.19 million additional people) was found over the 18.97 million captured in official episode-level reports for Pakistan, Bangladesh, and Sri Lanka. Over 460, 000 km² of agricultural land was exposed (18.5 % to >2m deep water), having significant implications for the region's predominantly agrarian economy.

Across publicly unmonitored regions and flood episodes, an estimated 237 million flood-exposed people were left in a data vacuum, completely missing from publicly-available mapping. Functionally, 22,818 low-lying healthcare facilities were inundated (3,041 functionally disrupted), severing last-mile care for 46.79 million people, including 28.54

Preprint not peer reviewed

This preprint research paper has not been peer reviewed. Electronic copy available at: https://ssrn.com/abstract=7353571

million exposed to deep-water flooding (>2m). In each country, access to at least 5% healthcare facilities was disrupted. Our rapid monitoring of the July–August 2026 crisis has already reported 11,905 km² of inundation, 92,140 km of submerged roads, 5.19 million exposed people including 1.6 million children (30.8%), and disruption to 1,900 basic health units, community clinics, pharmacies, and hospitals.

Interpretation

This first region-wide, multi-year study demonstrates that current global disaster response relies on severely incomplete or inaccessible data, effectively disenfranchising the world's most underserved and climate-vulnerable populations from healthcare when most needed. Rapid, reliable, and scalable precision intelligence is not a technical luxury but a necessary and achievable instrument for health equity and climate justice. To counter 21st-century global health threats, we recommend: (1) prioritising anticipatory planning for children and vulnerable communities via national action plans and community toolkits, (2) democratising disaster data through digital public infrastructure to inform equitable climate finance allocation, and (3) rapidly adopting precision surveillance in disaster intelligence frameworks to accelerate emergency response and safeguard health systems.

Funding This work was supported by Wellcome Trust Grant awarded to Sara Khalid [WT 313571/Z/24/Z]

Key words health resilience; digital public infrastructure; global health; universal health coverage; climate adaptation; loss and damage; remote monitoring; early warning

Preprint not peer reviewed

This preprint research paper has not been peer reviewed. Electronic copy available at: https://ssrn.com/abstract=7353571

Research in context

Evidence before this study

We searched PubMed, Google Scholar, and disaster databases (EM-DAT, ReliefWeb) for peer-reviewed articles and agency reports on methodological mapping, impact assessment, and operational assessments using combinations of "flood mapping," "hazard mapping," "satellite imagery," "remote sensing," "health," "education," "South Asia," "monsoon", "inundation," and "floods", focusing on studies in the six countries examined in our study. We reviewed key flood mapping methodologies and output from leading sources, namely the European Space Agency (ESA), United Nations Satellite Centre (UNOSAT), National Disaster Management Authorities (NDMA, DMC, NDRRMA, DDM), and UNDP Post-Disaster Needs Assessment (PDNA) reports published between 2020 and 2025.

Six systematic reviews were identified evaluating flood monitoring methodologies and damage assessment. While integrating remote sensing with machine learning in flood studies has been transformative for assessment and response preparation in South Asia, critical limitations still exist. Water observations of optical satellite sensors are blocked by persistent clouds during South Asia's monsoon season (June-October). Synthetic aperture radar (SAR) sensors are more suitable for monsoon conditions as they can penetrate atmospheric clouds day and night, but their output can misclassify water under dense vegetation in urban floodplains, or water flow during floods. Both sensor types suffer inadequate spatial coverage, temporal resolution constraints, and inability to measure real-time water levels at fixed points due to orbital cycles—thereby missing spatial precision needed for targeted response during floods. Further, disaster monitoring agencies rely on data are often proprietary or inaccessible.

Disaster risk scholarship and frameworks conceptualise flood impacts through the disaster risk chain, in which hazards interact with exposure, vulnerability, and capacity to produce impacts, such as service disruption, institutional fragility, and cascading or systemic risks across interconnected health, education, infrastructure, and supply-chain systems.

Two systematic reviews were identified on flood impacts on healthcare facilities and relevant mitigation strategies. Reviews consistently report that recent South Asian floods have affected tens of millions of people and inundated extensive areas.

Preprint not peer reviewed

This preprint research paper has not been peer reviewed. Electronic copy available at: https://ssrn.com/abstract=7353571

However, existing studies do not provide real-time exposure information on populations and on health and education facilities across South Asia, thereby limiting speedy response. The oft-widespread scale and unpredictable nature of floods necessitates versatile, scalable methods for accurate and time-critical information for prevention and management of ensuing public health crises.

Added value of this study

This study provides the first continuous, near-real-time, multi-country monitoring of flood impacts on public health infrastructure, overcoming critical operational and technological barriers. Across South Asia, the world's most populous region, our pipeline identified an additional 75 million mostly rural people and 22,000 healthcare facilities omitted from official surveillance reports, alongside sub-continent-wide impacts affecting over 250 million individuals. It is also the first to quantify direct flood exposure for nearly 90 million children in a region experiencing a rapid demographic shift toward youth aged under 30.

By generating daily reports within hours instead of weeks, our multi-modal remote sensing ensemble architecture bypasses technical cloud cover limitations and eliminates reliance on manual, time- and cost-intensive field surveys. Crucially, while existing surveillance captures only potential exposure-exent snapshots, our approach quantifies depth-based functional disruption—revealing that up to 11% of low-lying healthcare facilities across South Asia were rendered non-operational due to deep water. Field-validated during the 2025 floods and operationally deployed live in 2026, this work demonstrates that precision disaster surveillance is achievable at scale to safeguard healthcare delivery during emergencies.

Implications of all available evidence

Current surveillance methodologies offer an incomplete picture of disaster-induced public health paralysis. As urged by the UN Early Warnings for All initiative, adopting evidence-based, publicly accessible, continuous monitoring systems is essential to improve the speed and precision of anticipatory planning and emergency response. This enables targeted resource allocation to strengthen health systems where needed most, safeguarding universal health coverage and mitigating economic losses.

This preprint research paper has not been peer reviewed. Electronic copy available at: https://ssrn.com/abstract=7353571

A critical implication of our work is a three-fold recommendation: 1. Prioritise anticipatory planning to protect vulnerable, marginalised communities and children through national action plans and community toolkits. 2.Democratise health data by integrating real-time intelligence into digital public infrastructure, generating empirical evidence to quantify loss and damage for equitable climate finance allocation. 3. Adopt precision surveillance in disaster intelligence at scale to improve response speed, reduce preventable mortality and disease, and counter 21st-century anthropogenic global health threats.

Introduction

As the 2025 Lancet Countdown on Health and Climate Change warns, the incidence of extreme precipitation days, flash floods, and landslides has accelerated by 64% globally in the last 30 years of monitoring (1961 – 2024), fast outpacing resilience capability of healthcare systems around the world[3]. Flooding—defined as overflow of water onto normally dry land—is one of the most frequent and deadly natural hazards globally, irrespective of causes, depth, duration, or velocity. In 2020, it affected 3.2 billion people (41% of the global population), killing 218,000 individuals and causing economic losses exceeding US$1.3 trillion.[1,2] Flooding frequency increases annually, 21.1% of which is attributed to climate change, with a further 2.1% due to both climate and population increase.

However, the global response is jeopardised by a surveillance crisis. Authoritative flood maps produced by national and international disaster surveillance agencies are often inaccessible in practice for different reasons. These maps are generated only when activation is requested by a registered national authority; their release hinges on an affected government's consent to share data over their territories; and rely on cloud-vulnerable sensors.[22] Further, while some satellite data are open and free, the high-resolution imagery required for granularity and precision is typically commercial and licence-restricted.

In South Asia, home to a quarter of the world's population and one of the most climate-vulnerable regions prone to devastating floods, the traditional 'snap-shot' approach to disaster mapping poses an information hierarchy. Flood maps as not always publicly available, and production tends to be event-triggered. Resource-limited operations are often focused on economically important urban regions while remote rural areas risk being marginalized. Because the populations rendered invisible are typically those already lacking clean water and

This preprint research paper has not been peer reviewed. Electronic copy available at: https://ssrn.com/abstract=7353571

primary care, this information asymmetry fundamentally threatens health equity, universal health coverage (UHC), and monitoring the Sendai Framework commitments.

Home to the Hindukush-Himalaya glacial rooftop, and the Indus and Ganges River Systems (most densely populated in the world), the region experiences a 40% flood occurrence rate of riverine, flash, urban, icesheet melts, and monsoon floods and is the most vulnerable to monsoon deluges, which affect more people and larger areas than any other flood type.[4] Some floods resolve quickly, while others cause sustained inundation, where water fully covers lands at higher depth for an extent of time. Floods can also cause submersion of land and infrastructure at depths sufficient to endanger life and damage infrastructure. These seasonal events are caused by intense rainfall during the June-October monsoon season combined with glacial melt and transboundary river flows. Such floods are likely to keep increasing in frequency and severity in the future due to the region's downstream position in the surrounding river systems and melting icesheets, which is accelerating due to climate change.

Beyond the immediate loss of life and property, flooding disrupts human capital via the interruption of critical services such as healthcare[5,6] and education[7–10] via damage, or the hindering of access, to hospitals, clinics and schools.

A recent systematic review found that flood and cyclone-related flood hazards impacted healthcare facilities through flooded basements, service disruption, power and water interruptions, and evacuation needs, while confirming inconsistent disaster preparedness and necessary improvement.[11] Underestimation of flood inundation risk and inadequate preparedness compounds health risks not only by amplifying disease burden but also by impairing access to care when it is most needed.[12] Floods are associated with a range of health risks including: drowning, hypothermia and injury from submersion, skin and gastrointestinal infections from contaminants, damage to sewers, and waterborne diseases;[13] and in the longer term, food insecurity from inundation damage to crops,[14] and child malnutrition and stunting.[15] Furthermore, damage to roads and infrastructure impairs the distribution of food and medical supplies, transportation in emergency vehicles, and mobility of essential services.[13] A systematic literature review of mitigation strategies highlights the need to strengthen health system resilience using a multifaceted approach including engineering, managerial, social, and technological interventions, including facility elevation to prevent inundation, flood-hazard mapping, vulnerability assessment, resilient infrastructure design, emergency planning, and community engagement.[16]

This preprint research paper has not been peer reviewed. Electronic copy available at: https://ssrn.com/abstract=7353571

Downstream impacts include and may not be limited to crop-loss induced food insecurity, poverty and malnutrition. A metanalysis of the effect of climate variability, drought and flooding on malnutrition found that one of the most significant factors moderating the effects of climate variation in relation to malnutrition is age, with younger children (and older adults) the most susceptible.[17] Rodriguez Llanes et al (2011) show that flood-exposed children in rural India were 86% more likely to be stunted than flood-unexposed children, with a statistically significant difference.[18] These human and social vulnerabilities can translate into major economic consequences. The cascading effects—from loss of productivity to the collapse of health and education networks—compound inequality and slow recovery.

Systematic reviews show an uptake in flood disaster studies, flood hazard mapping, and flood inundation mapping that integrate remote sensing with artificial intelligence.[19–22] Such approaches can have transformative effects on early detection, accurate mapping, vulnerability assessment, decision support, community engagement, and cross-border collaboration.[20] However, in practice there are critical technological and operational gaps, especially in data - scarce and resource-limited countries and regions.[20,23] Water observations of optical satellite sensors are blocked by persistent clouds during South Asia's monsoon season (June-October).[22] SAR remote sensors can penetrate atmospheric clouds both day and night, thus are more suitable for monsoon condition; however, their output can misclassify water under dense vegetation in urban floodplains, or water flow during floods.[22,24] The ensuing limited adequate spatial coverage, temporal resolution constraints, and ability to measure real-time water levels at fixed points due to orbital cycles reduces spatial precision needed for targeted response during floods.[22,25]

Disaster risk scholarship and frameworks, including the Sendai Framework, conceptualise flood impacts through the disaster risk chain, in which hazards interact with exposure, vulnerability, and capacity to address impacts,[26] such as service disruption, institutional fragility, and cascading or systemic risks across interconnected health, education, infrastructure, and supply-chain systems.[27]

In this context, informed decision-making by both those delivering peri-disaster response and the affected communities themselves, requires near-real-time data: daily reassessments of the extent of flood inundation, exposure of health and educational facilities (at an individual hospital and school level), together with exposure of road infrastructure and crops, from national down to a local level. Further, identifying the extent of inundation exposure necessitates generalizable, scalable, and timely methods for high-precision identification of

This preprint research paper has not been peer reviewed. Electronic copy available at: https://ssrn.com/abstract=7353571

disaster locations and impacts. This study demonstrates that it is possible to provide a comprehensive picture of flood-caused water inundation in such a contemporaneous fashion, using geo-spatial data supplemented by AI in a region with the most intense monsoon season floods, extreme rain, and cyclones.

This paper seeks to address these operational and technological barriers. For the first time, to our knowledge, we designed, tested and validated an approach for near-real time continuous monitoring focused on preventing healthcare disruption . We designed and validated it across six South Asian countries during the entire 2025 floods season (most populous region in the world). It is currently deployed to monitor the ongoing 2026 floods season. We demonstrate that precision-surveillance nowcasting capability, operating at the speed, scale and spatial resolution required, is achievable and can identify functionally disrupted facilities, ultimately improving increase healthcare systems resilience and health equity, and recommend its incorporation in national adaptation plans and in digital public infrastructure in South Asia and beyond.

Methods

We first performed a continuous estimation of the inundation extent, depth, and type of flooding in 2025 in six countries of South Asia, namely Pakistan, India, Bangladesh, Bhutan, Nepal, and Sri Lanka, comparing our estimates with national and UNOSAT flood reports, where available. Due to the dynamic nature and variable causes of flooding, we considered flooding events including and not limited to flash, monsoon, landslide, riverine, urban, and compound events. The images captured in our methodology capture the presence of water on a surface at the moment of image capture and pre-event, enabling us to capture the inundation extent.

Next, we estimated potential exposure of the following: populations, health and education facilities, built-up and road infrastructure, as well as affected agricultural cropland. Results were updated in sync with satellite revisit times throughout the peak flood season of 2025, enabling continuous near-real time estimates to be produced.

Preprint not peer reviewed

This preprint research paper has not been peer reviewed. Electronic copy available at: https://ssrn.com/abstract=7353571

Continuous monitoring of inundation extent

We processed satellite data, observed every 1-2 days, from six synthetic aperture radar and optical satellite sensors**,** and provided it as input to a tailor-made model for pre- and post-flood change-detection to identify flood regions. Full details of the ensemble model architecture and flood detection framework are in the Appendix pp 4-8.

In brief, for each sensor (Sentinel-1 C-SAR, Harmonized Landsat-Sentinel [HLS] Landsat-30 OLI and MSI, Sentinel-2 MSI, Terra MODIS, Aqua MODIS, and S-NPP VIIRSS), cloud-free pre-flood and post-flood composites were generated over defined baseline and event periods. Sensor-specific flood indicators were derived using physically appropriate change metrics, including backscatter reduction for SAR and changes in water-sensitive spectral indices ((Normalized Difference Water Index (NDWI), Modified Normalized Difference Water Index (MNDWI), and Automated Water Extraction Index (AWEI)) and vegetation or brightness measures for optical sensors. Permanent surface water was excluded using a global water occurrence JRC mask to isolate transient inundation. Binary inundation maps from individual sensors were then combined into composite maps using ensemble strategies, including union, intersection, and majority voting, and a confidence surface reflecting the number of sensors detecting flooding at each pixel. This approach leverages the complementary strengths of radar and optical observations to improve flood detection robustness across heterogeneous landscapes and variable atmospheric conditions.

We validated the resulting maps showing inundation extent anomalous relative to a pre-event baseline with in-country field experts from national and provincial disaster management authorities who independently reviewed identified flood events and rectified the inundation extent boundaries against available on-ground observations. We further used UN-verified ReliefWeb reports and from Reuters media reports to determine how well our model estimated widespread as well as hyper-localised flooding events particularly in remote and hard-to-reach terrains e.g. mountainous regions.

Where available, UNOSAT maps were combined with our inundation maps to produce comprehensive coverage of inundation extent. Finally, four independent hydrometeorological datasets were used to assess consistency of detected flood events: the satellite-derived inundation maps were reviewed against hydrological models from Global Flood Awareness

This preprint research paper has not been peer reviewed. Electronic copy available at: https://ssrn.com/abstract=7353571

System4 (GloFAS[33]), CHIRPS3 v3.0[34], and MSWEP[35] for daily river discharges and total accumulated precipitation in the regions under study.

Complete Methods are described in Appendix pp 4-8 in detail.

Continuous estimation of population and infrastructure exposure

Population and infrastructure exposure refers to the spatial presence of people, infrastructure, ecosystems, or assets in places where they could be affected by a hazard, such as a flood. To quantify potential risk of exposure (hereafter referred simply to as exposure) of communities and infrastructure of living within the flood areas identified in our maps we integrated openly available basemaps from WorldPop for population, and OpenStreetMap for hospitals, schools, road networks, crops and built-up infrastructure[28–30]. WorldPop provides population maps derived from national census reports, whereas OpenStreetMap provide crowd-sourced data. These publicly available resources enabled the application of our proposed method for all countries and events of interest without reliance on proprietary data.[28–30] We then produced intersections of these static base maps with our continuously updated inundation maps to locate and quantify in near real-time potentially exposed total populations, subset populations at different age groups including children under 18 years, health and education facilities, and road infrastructure during 2025 in the six South Asian countries. We measured impacts in rural/urban areas classified according to GHS-SMOD degree of urbanization, and we stratified by flood types and month.

In-country Validation

We undertook quantitative validation in Pakistan, Sri Lanka, and Bangladesh based on the availability of publicly available episode-based UNOSAT inundation maps for the same geographies and timeframes. In Pakistan and Sri Lanka we were able to conduct additional field-verification of the models and maps through field visit conducted by the provincial disaster management authorities.

Continuous monitoring of deep-water exposure and functional disruption

To assess potential disruption within inundated areas, we estimated flood depth by measuring deep-water inundation across the region above a certain depth threshold, combining Earth Topography 1 Arc-Minute (ETOPO1[36]) elevation, the observed flood extent (coverage

This preprint research paper has not been peer reviewed. Electronic copy available at: https://ssrn.com/abstract=7353571

fraction), and the JRC RP10y depth layer masked to the Floodwater Depth Estimation Tool (FwDET[37])-derived footprint. We selected a 1.5-meter flood depth as a reasonable threshold above which facilities are functionally disrupted, based on experiences of national disaster authorities in the region. We also applied a 2-meter flood depth threshold to increase reliability of our assessment.

There is no universal reporting standard for the flood depth at which infrastructure ceases to function, hence we defined disruption thresholds on the basis of technical reasoning and regional building characteristics and disaster-management practice. Operative depth values vary with regional topography and development type; however, depth–damage functions consistently show that damage and disruption increase sharply with depth (Huizinga et al., 2016; Merz et al., 2010). The 1.5-meter threshold was selected as the primary threshold as in Pakistan and comparable South Asian contexts, ground-floor ceiling heights typically range from 2.1 to 3.0 m (7–10 feet), such that inundation of 1.5 meter submerges the majority of the ground floor and can be expected to compromise access and egress, electrical systems, sanitation, equipment, and basic service continuity. This threshold is consistent with operational guidance from the Provincial Disaster Management Authority (PDMA). Given the uncertainty inherent in combining the elevation, flood-coverage, and depth-modelling inputs, we applied a 2-meter threshold as a sensitivity analysis, yielding a conservative, higher-confidence estimate of disruption at the cost of potentially undercounting facilities already non-functional at shallower depths.

These depth-threshold masks were generated to entail that functional disruption can be mapped in near-real-time and nowcast as events evolve.

Stakeholder and community co-design

To evaluate potential policy implications and community-level operational implementation, this work was co-designed with national public health policymakers, disaster management authorities, and community groups. Specifically, a multilateral stakeholder workshop was conducted for qualitative validation of the findings and potential integration into disaster risk reduction and public health guidelines.

Compute was performed using Google Earth Engine, a cloud-based platform that enables large-scale analysis of remote sensing data, and QGIS v 3.44 (Appendix pp 8).

Preprint not peer reviewed

This preprint research paper has not been peer reviewed. Electronic copy available at: https://ssrn.com/abstract=7353571

Live near-real-time deployment and validation during the ongoing 2026 monsoon season

To demonstrate operational utility during an active emergency, we applied the pre-validated 2025 pipeline in near-real time to the ongoing 2026 South Asian floods season, during July-August. We emphasise that this is a live monitoring deployment – or nowcasting – of an event still in progress, not a forecast or hindcast. The completed 2025 season provides the methodological baseline, replicated across all six countries, whereas the 2026 outputs are continuous updates, reported here as of 1 August 2026. At the time of writing, the floods season is ongoing, all 2026 exposure figures are provisional lower bounds that will rise as the floods continue. In-house reviews by UN OCHA and Punjab Disaster Management Authority officials confirmed results on the ground consistent with those of our 2026 modelling.

With floods ongoing, we conducted targeted ground verification along the Ravi River corridor (Lahore and Narowal districts, Punjab, Pakistan) against eight monitoring points reported by the Provincial Disaster Management Authority (PDMA).

Results

Continuous estimation of inundation extent in 2025

From June to December 2025, a total of 242 flood events were observed and field-verified, across Pakistan, India, Bangladesh, Nepal, Bhutan, and Sri Lanka (**Figure 1**) using the proposed inundation extent detection and validation pipeline (**Figure 2**).

Field verification confirmed these events to include 77 riverine flooding, 61 flash flooding, 19 flash/monsoon/landslide (compound), 10 riverine/monsoon/urban (compound), 7 riverine/monsoon/landslide (compound), 25 urban flooding, 14 landsliding, 8 coastal flooding, 17 cyclone-related floods, 1 glacial lake outburst flood (GLOF), and 3 monsoon flooding events (**Figure 1**).

These events were driven by intense monsoon rain resulted in fatal flooding across Pakistan, India, and Nepal, damaging critical infrastructure and farmland, as well as "cloudburst" events, in addition to La Niña influence resulting in above-average rainfall which intensified the risk of flooding and landslides. Extreme precipitation anomalies were confirmed by GloFAS-CHIRPS-MSWEP maps.

Preprint not peer reviewed

This preprint research paper has not been peer reviewed. Electronic copy available at: https://ssrn.com/abstract=7353571

The total inundation extent observed across South Asia was 6.89 x 10^5 km² (15%) (**Table 1**). India accounted for the largest inundated area (541,342.6 km², 16%), followed by Pakistan (114,513.0 km²,13%) and Bangladesh (20,922.2 km², 14%). Smaller flooded areas were observed in Nepal (8,614.0 km², 5.8%), Sri Lanka (3624 km²,5%), and Bhutan (714.8 km²1.8%).

In comparison, publicly available UNOSAT maps reported flood episodes in just 3 of the 6 countries under study, namely 7,000, 3,600, and 13,900 km² for Pakistan, Sri Lanka, and Bangladesh, respectively. Our model independently detected each of these individually reported episodes, agreeing with UNOSAT estimates for episode-level inundation extent (**Table 1**). Publicly available UNOSAT inundation maps were not found for India, Bhutan, and Nepal.

Our continuously measured inundation maps when combined with these existing episode level UNOSAT maps increased the total estimated extent from June to Dec 2025 to 6.89 × 10^5 km², reflecting an overall 19-fold increase in inundation extent coverage (**Table 1**).

Below we present two highly-localised case studies, demonstrating how the technique is applicable in a wide variety of scenarios ranging from abrupt land slide events in remote mountainous terrains, slow moving riverine floods, and composite urban flash floods.

Nowcasting urban flash flood and remote landslide exposure (August–September 2025)

Daily nowcasting of the August–September 2025 monsoon hazard chain demonstrates the operational value of the framework. In downstream Punjab, derived flood masks captured the onset, peak, and recession of Chenab riverine inundation across Sialkot district, while upstream in Khyber Pakhtunkhwa the same daily pipeline resolved two distinct pulses of flash-flood and GLOF activity co-located with landslide detections along the Swat, Panjkora, and upper-Indus corridors. Together these products link downstream inundation to its upstream convective and cryosphere triggers within a single time-resolved hazard chain. **Figure 5** and **Figure 6** illustrate two examples of nowcasting an urban flash flood event and landslide in remote mountain regions, respectively.

We examined downstream riverine/urban inundation in Sialkot district, Punjab, linked to upstream mountain flash floods, GLOFs, and landslides in Khyber Pakhtunkhwa. From 25 August to 14 September 2025, daily derived flood masks for Sialkot district in downstream Punjab (**Figure 5**) show riverine inundation first detected on 27–28 August, expanding rapidly

This preprint research paper has not been peer reviewed. Electronic copy available at: https://ssrn.com/abstract=7353571

through 3–5 September as the Chenab crest propagated, and contracting after 11 September; the cumulative wetted area reached 863·9 km² (28·0% of district area), with persistent water concentrated at the Chenab–Ravi confluence and along low-lying floodplain sub-basins.

Upstream in mountainous Khyber Pakhtunkhwa, the monsoon hazard signature evolved in two distinct pulses across the August–September period (**Figure 6**). Flash-flood and glacial-lake-outburst flood (GLOF) activity was sparse during the first fortnight, escalated abruptly during the 16–20 August cloudburst, and reached its first peak on 16–25 August (1,241 km²) before a second, broader peak on 5–9 September (1,604 km²); co-located landslide detections tracked these pulses but at more than two orders of magnitude smaller area. The cumulative 50-day footprint reached 2,866 km² of flash-flood and GLOF-affected terrain (~18·6% of the six-district region) and 12·8 km² of landslide scars, concentrated along the Swat, Panjkora, and upper-Indus corridors.

Together the two examples illustrate the ability to detect highly-localised abrupt heterogenous events in both populous riverine centres and remote rural regions, including hard-to-reach mountainous terrains.

Continuous estimation of population, agriculture, and health infrastructure exposure in 2025

Population

Across the six countries in South Asia, a total of 257.67 million people (13.3% of the region's population) were potentially exposed to floods between June and December 2025 (**Table 2**). This includes 65.71 million (26% of the country's population) in Pakistan, 160.75 million (11%) in India, 22.24 million (12.74%) in Bangladesh, 5.66 million (19.12%) in Nepal, 0.082 million (10.38%) in Bhutan, and 3.21 million (13.85%) people in Sri Lanka.

The exposed population included a total of 89.3 million (14.5%) boys and girls aged under 18 across the six countries, including 28.65 million (26.3% of the country's children) in Pakistan, 50.04 million (11.6%) in India, 7.62 million (12.95%) in Bangladesh, 2.90 million (21.04%) in Nepal, 0.02 million (9.85%) in Bhutan, and 0.88 million (14.36%) in Sri Lanka.

Existing UNOSAT episode-level reports, which reported population exposure for Pakistan, Bangladesh and Sri Lanka flood events, covered a total of 18.97 million people (**Table 1**). In comparison, our continuous monitoring estimated a total of 91.16 million from just these 3

This preprint research paper has not been peer reviewed. Electronic copy available at: https://ssrn.com/abstract=7353571

503 countries (4-fold or 72.19 million more (**Table 2)**). Publicly available UNOSAT reports were
504 not found for India, Nepal, and Bhutan.

505

506 ## Agricultural Cropland

507 A total of 462,160 km² of agricultural cropland was included in the flooded regions, spread
508 across India (368,725 km²), Pakistan (67178 km²), Bangladesh (17,455 km²), Bhutan (22 km²),
509 Nepal (270 km²) and Sri Lanka (4,323 km²) (**Table 3**).

510 With 59% cropland exposed, Sri Lanka was the most disproportionately affected. Other
511 countries with more than 20% damage cropland included Pakistan (33%), India (29%),
512 Bangladesh (25%) and Nepal (27%). Whereas in Bhutan had 12% of cropland damaged.

513

514 ## Infrastructure: health & education facilities, roads, and built-up areas

515 In total, 13,937.23 thousand km² built-up infrastructure was affected across the region,
516 including residential, commercial and industrial structures (**Table 3Table 3**).

517 This included an estimated 22,818 (15.3%) healthcare facilities across the region. This included
518 but was not limited to community clinics and basic health units, pharmacies, and primary and
519 secondary care hospitals. At least 5% health facilities were exposed in each country (**Figure 8,**
520 **Appendix Figures S6 & S7**).

521 Similarly 7,887 (14.9%) education were estimated including pre-school or kindergarten
522 locations, primary and secondary schools, colleges and universities.

523 Additionally, 75.52 thousand km² roads were affected in total across the region, further
524 exacerbating access to abovementioned education and healthcare facilities.

525 # Estimation of functionally disrupted population and infrastructure in
526 2025

527 Across the six countries, 458,495.1 km² was inundated to depths exceeding 1.5 meters (**Figure**
528 **3**), two-thirds (66.5%) of the total observed inundation extent and 11% of the region's total
529 land area, of which 227,259.6 km² exceeded 2 m **(Table 4).** India accounted for the largest
530 deep-water extent (358,374.6 km², 10.6% of the country's area at >1.5 m), followed by Pakistan

This preprint research paper has not been peer reviewed. Electronic copy available at: https://ssrn.com/abstract=7353571

(77,047.2 km², 8.8%) and Bangladesh (13,783.4 km², 9.2%), with smaller extents in Nepal (6,558.0 km², 4.4%), Sri Lanka (2,149.0 km², 3.0%), and Bhutan (582.9 km², 1.5%).

A total of 46.76 million people (18.1% of the flood-exposed population) were potentially exposed to inundation deeper than 1.5 m, of whom 28.54 million were exposed to depths exceeding 2 m (**Table 5**). Pakistan had both the largest relative and second-largest absolute deep-water population exposure (16.59 million, 6.6% of the national population at >1.5 m), alongside India (26.25 million, 1.8%), Bangladesh (3.39 million, 1.9%), Nepal (0.35 million, 1.2%), Sri Lanka (0.18 million, 0.8%), and Bhutan (0.017 million, 2.2%). Children and adolescents under 18 exposed to functionally disruption depths reached 17.19 million (>1.5 m) and 10.26 million (>2 m), with Pakistan being the most affected (7.41 million children, with 6.8% of the country's under-18 population exposed at depth >1.5 m) (Appendix pp 10-14).

Disruption to health and education services carries consequences beyond the immediate flood period. Across the region, 3,041 hospitals were located in water deeper than 1.5 m, of which 2,119 were in water deeper than 2 m depths at which facilities are rendered inaccessible to patients and staff, and at which ground-floor wards, equipment, cold chains, and power supplies are liable to fail precisely when flood-related injuries, waterborne and vector-borne disease, and interrupted care for chronic conditions increase demand. India accounted for the majority of affected facilities (2,717 at >1.5 m), followed by Bangladesh (143) and Pakistan (108). A further 1,047 schools were situated in water deeper than 1.5 m (759 deeper than 2 m), led by India (634), Nepal (153), and Bangladesh (133).

Potential disruption to physical infrastructure and livelihoods was substantial (**Table 4** and **Table 5**). Deep water (>1.5 m) covered 1,981.9 km² of built-up area, 84,985.8 km² of cropland, and 24,337.7 km of roads across the region, falling to 1,299.5 km², 54,700.9 km², and 16,764.5 km, respectively, at the 2 m threshold. Cropland disruption was concentrated in India (62,097.7 km², 4.9% of national cropland at >1.5 m) and Pakistan (18,835.2 km², 9.1%), while relative road-network disruption was highest in Bangladesh (8,752.8 km, 2.3%), Sri Lanka (2,729.3 km, 2.2%), and the mountainous networks of Nepal (4,911.9 km, 1.7%) and Bhutan (484.5 km, 1.7%), where severed corridors compound isolation of remote communities.

The urban–rural distribution of deep-water disruption differed markedly from that of overall inundation (**Figure 4**). Whereas overall flooding intersected 41.5–74.6% of urban regions and 25.5–64.7% of rural regions across the six countries, deep-water conditions were confined to a far smaller subset: 7.7–21.4% of urban regions at >1.5 m (highest in Bangladesh, 21.4%; Nepal

This preprint research paper has not been peer reviewed. Electronic copy available at: https://ssrn.com/abstract=7353571

and Sri Lanka, 18.6% each) and 2.9–11.4% of rural regions (highest in Bangladesh, 11.4%; India, 8.7%). Bangladesh exhibited the greatest deep-water penetration in both settlement classes, with 18.2% of urban and 7.9% of rural regions intersected even at the 2 m threshold, consistent with its low-lying deltaic geography.

Overall trends

Our analysis revealed a critical gap in current surveillance. In 2025, continuous monitoring identified 257.67 million (**Table 2**) exposed individuals (29.1% in rural areas (**Appendix Table S13**)) including 89.3 million children under 18. A five-fold increase (72.19 million additional people (**Table 2**)) was found over the 18.97 million (**Table 1**) captured in official episode-level reports for Pakistan, Bangladesh, and Sri Lanka. Over 460, 000 km² of agricultural land was exposed (18.5 % >2m deep water), with serious ramifications for the region's predominantly agrarian economy.

Over a quarter of all children under 18 were exposed in Pakistan, and between 10% - 26% across South Asia. In all countries at least 5% healthcare facilities were affected. Sri Lanka was the most highly affected with regards to road network exposure (21%), Bangladesh (20.2%) and Nepal (19%) with regards to built up infrastructure, and Pakistan with respect to cropland exposure (39%). By area, over a tenth of South Asia was exposed to deep water (1.5- 2m), implying potential displacement of 28- 46 million people, including of 10-17 million children. 22000 health facilities were exposed of which over 2000 risked functionally disruption.

Overall, through continuous monitoring over a period of 6 months in 2025, we detected 12-fold greater flooded inundation area than previous episode-level reporting (**Table 1**), through which we identified over 200 events in urban, rural, and remote locations of South Asia. In Pakistan, Bangladesh, and Sri Lanka alone we identified 75 million exposed rural people missed by episode-level reports.

Live near-real-time monitoring of 2026 emergency, as of 12 August 2026

Deploying live during 23–28 July of the ongoing 2026 floods season showed a regional inundation footprint of 11,905 km² across the six countries. As of 12 August 2026, 5,193,295 people, of whom 1,697,722 (approximately 32.7%) were children under 18 were found to be exposed. Across the region, 1,900 healthcare facilities (hospitals, pharmacies, and basic health units) and 618 schools were functionally disrupted, and 92,140 km of roads were submerged. These figures describe an emergency still in progress and are therefore provisional (**Figure 7**).

Preprint not peer reviewed

This preprint research paper has not been peer reviewed. Electronic copy available at: https://ssrn.com/abstract=7353571

Country-level results present further insights. Our results showed India had the largest inundated area (6,820 km²), exposing 2,195,958 residents (639,245 children), with 1,703 hospitals within flood boundaries and 49,347 km of roads affected. Bangladesh had the highest relative population impact (1.56% of the national population; 2,724,949 people, including 941,062 children), with a heavily urban footprint (86.9%) and 26,285 km of roads submerged (5.28% of the national network). In Pakistan, 221,571 people were exposed (101,141 children) across 1,421 km² (53.1% rural), with 21 hospitals, 14 schools, and 10,745 km of roads affected. Smaller but locally acute impacts were recorded in Sri Lanka (35,856 people, 80.8% urban; 33 hospitals, 109 schools), Nepal (14,699 people; 144 schools), and Bhutan (262 people; 8 km²; 359 km of roads).

Field-verification along the Ravi River corridor of the Indus River System exposed a critical operational blind spot: standard automated 100 m flood-extent products detected none of the eight PDMA-confirmed inundated sites, since such products are tuned to wide riverine overbank flooding and systematically under-detect the short-duration, high-intensity pluvial pooling that dominated this event. In direct contrast, our approach returned strong positive shifts in the Normalised Difference Water Index (ΔNDWI +0.100 to +0.372), confirming new standing water, with modelled depths of 0.23 m to 1.60 m.

Stakeholder consultation findings

As part of this study, we undertook an informal stakeholder consultation with national, and community actors, including senior representatives of the regional networks from each of the 6 countries, public health experts, and disaster management officials. Stakeholders during the consultations noted the value of these type of data and algorithms for disaster preparedness and response. Disaster management representatives noted that the approach can reduce inundation mapping time from one month to around 30 minutes, significantly improving early warning systems, resource mobilization, and pre-emptive relocation of vulnerable populations. An official based in a Himalayan surveillance station emphasized its usefulness in poorly monitored rural and mountainous areas, which are otherwise unseen to people in the capital leading on national level disaster response. Regional network members recommended integration of results directly in child-focused disaster planning and decentralized services such as mobile crèches, and that the near–real-time identification of affected health and education facilities can guide evacuation and service continuity decisions. Overall, stakeholders stressed

This preprint research paper has not been peer reviewed. Electronic copy available at: https://ssrn.com/abstract=7353571

627 the method helps fill gaps in existing disaster frameworks—particularly focused on the
628 youngest and most vulnerable —and enables relief to protect health and education outcomes.

629 The issue of mis-information was raised – it is often difficult to know to whom to turn and who
630 to trust in a widespread crisis. Access to reliable and timely information of the type detailed
631 above can help communities filter out misinformation that in the past has generated panic
632 among local populations, especially children. They suggest that authority-generated alerts
633 could be communicated to the community via trusted religious leadership and community
634 centres. Finally, they reflected on the desirability for the future integration of micro-level and
635 children and adult lived experience of flooding into data collection efforts.

636 Discussion

637 This study provides a continuous near real time picture of major flooding and its acute
638 humanitarian and public health impact, quantifying interlinked population, agricultural, and
639 healthcare infrastructure exposure, differentiating by age groups, and particularly in
640 marginalised communities, living in remote/rural/urban areas, accounting for flood type, and
641 month, highlighting acute, indirect, and downstream ramifications. To our knowledge these are
642 the first publicly available season-long and monthly inundation maps across the six countries
643 with corresponding exposure estimates for all of them. We deliver near–real-time inundation
644 extent and exposure estimates for total and sub-populations, health and education facilities, and
645 road infrastructure during 2025 across the six south Asian countries, demonstrated
646 operationally via near real-time monitoring of one episode during the ongoing 2026 monsoon
647 crisis.

648 Taken together, the 2025 and 2026 analyses carry three primary public health messages.

649 First, there is a major surveillance gap that indicts the status quo. We detected 242 field-verified
650 flood events were in 2025, of which only 5% were captured by existing reports due to lack of
651 or missed reporting. To be among the invisible population in a disaster database is to be
652 invisible to the humanitarian supply chain and the climate adaptation budgets.

653 Second, the burden falls disproportionately on the youngest and most vulnerable. Of the 257.67
654 million (13.3%) million population exposed in 2025, 89.3 million were children exposed in
655 2025, and 5.19 million people including nearly one-third (1.7 million) children in in July 2026.
656 In Pakistan, over 1 in 4 children (26%) were caught in the flood zones.

Preprint not peer reviewed

This preprint research paper has not been peer reviewed. Electronic copy available at: https://ssrn.com/abstract=7353571

Third, data poverty compounds health inequity and erodes health-system resilience. The 75 million people we identified as 'missing' are often the same populations lacking clean water and primary care. We mapped 7,887 educational facilities and 22,818 health facilities inundated in 2025, and 1,900 health facilities and 618 schools exposed in July 2026 alone, which marks an alarming live, still-rising snapshot of an emergency in progress. We identified over 21,000 exposed health facilities in 2025 in India alone which were previously unmapped.

The 2026 results sharpen this argument. Within a single week of an ongoing crisis, and reported live as of 1 August 2026, our methodology identified cumulative, cross-border figures that episode-based reporting does not assemble. Just as importantly, the failure of standard automated 100 m products to detect any of the eight ground-confirmed Ravi-corridor sites exposes a dangerous surveillance blind spot precisely where health authorities most need situational awareness. The 2025 results have validated our method across six countries, while the 2026 results demonstrate that our method can be used live during an emergency without forecasting or extrapolating beyond what has already been observed.

Inundation of the aforementioned healthcare facilities, 3,041 of which in water deep enough to compromise function, represents a systemic collapse of the health delivery system and catastrophic interruption of continuum of care. When road networks (75,520 km) fail alongside clinics, the last mile of care is severed for precisely those populations least able to travel further. We argue that near-real-time, open-access datasets are not merely scientific tools; they are instruments of climate justice. To that end, we have made our outputs available through a publicly accessible, near-real-time dashboard, and have begun sharing them directly with national disaster management authorities, at the time of writing, with Pakistan and Sri Lanka. By democratizing this information, we may hope to empower local communities to move from being passive victims of 'undetected' floods to active participants in an anticipatory, resilient health system.

As extreme weather events intensify and populations grow in flood-prone low- and middle-income countries, scalable and speedy technology for pre- and post-disaster intelligence are increasingly critical. Our study addresses this need by integrating remote sensing from six synthetic aperture radar and optical satellites with an AI-based pre- and post-event change-detection framework, validated against expert field analysis and news reports. Past floods have shown that the full toll has yet to be determined, including mortality, the full extent of damage to crops exposing millions of people at risk disease and malnutrition.

This preprint research paper has not been peer reviewed. Electronic copy available at: https://ssrn.com/abstract=7353571

Estimating exposure to functional disruption offers a critical measure for assessing severity of damage. Beyond interrupted health care and schooling, these facilities typically double as evacuation shelters and vaccination or nutrition delivery points in flood-prone districts. As such, functional disruption compounds public-health and educational harms caused by the floods and climate change.

Strengths: Our method provides specific information on flood locations at scale, including in remote mountainous areas with limited access, in almost real-time: VIIRS and MODIS sensors provide near-daily observations, while sensors from HLS offer ~2–3 day revisit and Sentinel-1 provides ~6-day all-weather coverage, in a format (free, downloadable) that can be accessed by everyone. Therefore, the effective revisit time of the integrated system is closer to near-daily (~1 day). Hitherto it has been extremely difficult—if not impossible—to attain these speed of rapid reporting, given the limitations of the current data and the scale of impacts. The value of this work is therefore to fill data gaps in a way that can provide real-time information for rapid, reliable and reproducible/scalable decision making to protect lives, to guide the humanitarian response, and prioritise healthcare facilities. In benchmarking results against existing inundation maps, our approach has identified riverine and flash floods that have not previously been identified in official single-level inundation maps, and in a timeframe of 30 minutes, a process for which authorities would have required one month.

Unlike humanitarian organisational products that are proprietary and limited, our data is open access for all, enabling local and national authorities to view near-real time flood information and exposure assessment at minimal costs, thereby facilitating accessibility to local groups and communities to inform local adaptation efforts. Moreover, these numbers can be used by governments to calculate loss and damage caused by the flooding, enabling insurance calculations to protect healthcare facilities and infrastructure.

Study limitations: Whilst our approach is designed to improve estimation of exposure to flood hazards thereby alerting to who is in harm's way, it did not distinguish risk by severity, duration, or recurrence, or vulnerability of those impacted and, therefore, the extent of potential harm caused.

Other than in Pakistan and Sri Lanka, it was not possible to access field-verified data. We have relied on publicly available data, some of which is crowd sourced, as in the case of location of hospitals, and schools. The implication is that our school and hospital exposure results may well be an underestimation of the proportion of hospitals and schools impacted. Second,

Preprint not peer reviewed

This preprint research paper has not been peer reviewed. Electronic copy available at: https://ssrn.com/abstract=7353571

dependency on satellite revisit times impacts frequency of continuous monitoring. Finally, we measure exposure and depth-thresholded functional disruption, not morbidity or mortality as the latter sensitive data were not reliably available. Fourth, the 2026 figures describe an emergency in progress, for the 23-28 July episode and reported as of 1 August 2026, and are thus provisional lower bounds that will rise as the catastrophic season continues.

Conclusion

Until now, officials in capital cities and local communities alike, in particular in low- and middle-income countries, had no way to see the full footprint of a flood season in hard-to-reach, rural and mountainous areas in the greatest hour of need. The consequences are measurable, as shown in our paper. While not escaping the floods, marginalised people are missing from the data on which relief, budgets, and adaptation finance depend.

Although expert-led, traditional manual field surveys remain time-consuming, expensive, and limited in scale. By combining satellite data with multi-modal AI, we have produced a comprehensive robust automated monitoring system, replicable in other countries to allow for the provision of continuous, near real-time monitoring of floods. As such it holds the potential for enhancing health resilience and peri-disaster response. This premise is evidenced by successfully demonstrating our method for the ongoing 2026 floods, reported herein as of 1 August 2026.

We therefore argue that continuous, open, near-real-time flood surveillance should be treated as Digital Public Infrastructure and written into National Adaptation . Embedding it there converts disaster intelligence from a product issued to governments on request into a public service instrument available to the health workers, district officials, and communities who must act on it within hours.

Preprint not peer reviewed

This preprint research paper has not been peer reviewed. Electronic copy available at: https://ssrn.com/abstract=7353571

To that end, we conclude with a three-fold recommendation: 1. prioritisation of anticipatory planning to protect vulnerable, marginalised communities and children through national action plans and community toolkits. 2.democratisation of health data by integrating real-time intelligence into digital public infrastructure, generating empirical evidence to quantify loss and damage for equitable climate finance allocation. 3. adoption of precision surveillance in disaster intelligence at scale to improve response speed, reduce preventable mortality and disease, and counter 21st-century anthropogenic global health threats.

Declaration of interests

We declare no competing interests.

Contributors

Sara Khalid led the study, contributed to its conceptualisation and interpretation, provided scientific and public-health oversight, digital health expertise, critically reviewed and revised the manuscript and is overall responsible. **Usman Nazir** developed and implemented the multimodal satellite based analytical framework, conducted the data processing and statistical analyses, interpreted the results, and drafted and revised the manuscript. **Manal Shehabi** led the drafting and revision of the manuscript, developed policy analysis and implications, and contributed to the interpretation and framing of the findings. **Hamid Mahmood** contributed expertise in international space-based disaster information and Earth-observation applications, reviewed and interpreted the findings, and critically revised the manuscript. **Elizabeth Stuart** contributed to the interpretation and framing of the findings and drafted and revised the manuscript. **Rochelle Schneider** contributed expertise in Earth observation, geospatial analytics, remote sensing, and machine-learning applications, and critically reviewed and revised the manuscript. **Lalith Rajapakse** provided local hydrological and flood expertise and verification of the Sri Lanka results and critically reviewed the manuscript. **Muhammad Kamran** provided local hydrological and flood expertise and verification of the Pakistan results and critically reviewed the manuscript. **Aluisio Barros** contributed to the interpretation of the findings from a global health and health-equity perspective and critically reviewed the manuscript. **Jere Berman** contributed to the broader interpretation of the climate, economic, and societal implications of the findings and critically reviewed the manuscript. **Chemba Raghavan** contributed expertise in early childhood development and child-focused policy and

Preprint not peer reviewed

This preprint research paper has not been peer reviewed. Electronic copy available at: https://ssrn.com/abstract=7353571

interpretation and critically reviewed the manuscript. **Neven Fuckar** advised on climate and hydrology models and critically reviewed the manuscript. **Myles Allen** contributed expertise in climate science and interpretation of the relationship between extreme weather and climate change and critically reviewed the manuscript. **Alan Stein** contributed expertise in child and adolescent health and development and critically reviewed the manuscript. **Omnia El Emrani** contributed public health expertise and advocacy discourse. All authors reviewed and approved the final manuscript and agreed to be accountable for all aspects of the work. We submit this work on behalf of the Children and Climate Initiative consortium.

Data sharing

The satellite and ancillary datasets used in this study are publicly available from their respective data providers, including Sentinel-1, Sentinel-2, Harmonized Landsat–Sentinel, MODIS, VIIRS, WorldPop, OpenStreetMap, JRC Global Surface Water, ETOPO1, GloFAS, CHIRPS, and MSWEP. The UNOSAT and other publicly available flood-report datasets used for comparison are available through the respective provider platforms and cited sources. The derived flood inundation maps, exposure estimates, analytical outputs, and code used to generate the results will be made available in an open GitHub repository at publication. Additional processed data and analytical materials that cannot be deposited because of third-party licensing restrictions will be available from the corresponding author on reasonable request, subject to the applicable data-use conditions.

References

1 Liu Q, Du M, Wang Y, *et al.* Global, regional and national trends and impacts of natural floods, 1990–2022. *Bull World Health Organ* 2024; **102**: 410–20.

2 Shamsudduha M. Redefining flood hazard and addressing emerging risks in an era of extremes. *npj Nat Hazards* 2025; **2**: 29.

3 Romanello M, Walawender M, Hsu S-C, *et al.* The 2024 report of the Lancet Countdown on health and climate change: facing record-breaking threats from delayed action. *Lancet* 2024; **404**: 1847–96.

4 Hossen N, Nawaz S, Kabir H. Flood Research in Bangladesh and Future Direction: An Insight From Last Three Decades. *International Journal of Disaster Risk Management* 2022; **4**: 15–39.

Preprint not peer reviewed

This preprint research paper has not been peer reviewed. Electronic copy available at: https://ssrn.com/abstract=7353571

5 Yang Z, Huang W, McKenzie JE, *et al.* Hospitalization risks associated with floods in a multi-country study. *Nat Water* 2025; **3**: 561–70.

6 Ebi KL, Vanos J, Baldwin JW, *et al.* Extreme Weather and Climate Change: Population Health and Health System Implications. *Annual Review of Public Health* 2021; **42**: 293–315.

7 Venegas Marin S, Schwarz L, Sabarwal S. Impacts of Extreme Weather Events on Education Outcomes: A Review of Evidence. *The World Bank Research Observer* 2024; **39**: 177–226.

8 Gul S, Khalil I, Hidayat K. "Impact of 2022 flood on girls' education: A case study of District Nowshera, Khyber Pakhtunkhwa, Pakistan". *International Journal of Disaster Risk Reduction* 2024; **114**: 104988.

9 Khalid N, Behrman J, Hannum E, Thapa A. Floods and Children's Education in Rural India. *rsf* 2024; **10**: 230–54.

10 Marin SV, Schwarz L, Sabarwal S. Impacts of Extreme Weather Events on Education Outcomes: A Review of Evidence. *The World Bank Research Observer* 2024; **39**: 177–226.

11 Abebe YA, Pregnolato M, Jonkman SN. Flood impacts on healthcare facilities and disaster preparedness – A systematic review. *International Journal of Disaster Risk Reduction* 2025; **119**: 105340.

12 Rae M, Van Hove M, Göpfert A. Effect of climate related flooding on health and healthcare worldwide. *BMJ* 2023; : p1331.

13 Du W, FitzGerald GJ, Clark M, Hou X-Y. Health impacts of floods. *Prehosp Disaster Med* 2010; **25**: 265–72.

14 Pacetti T, Caporali E, Rulli MC. Floods and food security: A method to estimate the effect of inundation on crops availability. *Advances in Water Resources* 2017; **110**: 494–504.

15 Agabiirwe CN, Dambach P, Methula TC, Phalkey RK. Impact of floods on undernutrition among children under five years of age in low- and middle-income countries: a systematic review. *Environ Health* 2022; **21**: 98.

16 Arefi F, Tavan A, Moradi SM, Daneshi S, Farahmandnia H. Identifying challenges and future directions of flood hazards mitigation strategies in health facilities: a systematic literature review. *BMC Emergency Medicine* 2025; **25**: 174.

17 Lieber M, Chin-Hong ,Peter, Kelly ,Knox, Dandu ,Madhavi, and Weiser SD. A systematic review and meta-analysis assessing the impact of droughts, flooding, and climate variability on malnutrition. *Global Public Health* 2022; **17**: 68–82.

18 Rodriguez-Llanes JM, Ranjan-Dash S, Degomme O, Mukhopadhyay A, Guha-Sapir D. Child malnutrition and recurrent flooding in rural eastern India: a community-based survey. 2011; published online Jan 1. DOI:10.1136/bmjopen-2011-000109.

Preprint not peer reviewed

This preprint research paper has not been peer reviewed. Electronic copy available at: https://ssrn.com/abstract=7353571

19 Zhao J, Li M, Li Y, Matgen P, Chini M. Urban Flood Mapping Using Satellite Synthetic Aperture Radar Data: A Review of Characteristics, Approaches and Datasets. 2024; published online Nov 6. DOI:10.48550/arXiv.2411.04153.

20 Madushani JAT, Withanage NC, Mishra PK, Meraj G, Kibebe CG, Kumar P. Thematic and Bibliometric Review of Remote Sensing and Geographic Information System-Based Flood Disaster Studies in South Asia During 2004–2024. *Sustainability* 2024; **17**. DOI:10.3390/su17010217.

21 Amitrano D, Martino GD, Simone AD, Imperatore P. Flood Detection with SAR: A Review of Techniques and Datasets. *Remote Sensing* 2024; **16**. DOI:10.3390/rs16040656.

22 Tao Y, Tian B, Adhikari BR, Zuo Q, Luo X, Di B. A Review of Cutting-Edge Sensor Technologies for Improved Flood Monitoring and Damage Assessment. *Sensors (Basel)* 2024; **24**: 7090.

23 Romali NS, Sulong S, Kawasaki A. A Systematic Review of Flood Damage Assessment: Insight for the Data-Scarce Regions. *Water Resour Manage* 2025; **39**: 4707–34.

24 Twele A, Cao W, Plank S, Martinis S. Sentinel-1-based flood mapping: a fully automated processing chain. *International Journal of Remote Sensing* 2016; **37**: 2990–3004.

25 Shen X, Wang D, Mao K, Anagnostou E, Hong Y. Inundation Extent Mapping by Synthetic Aperture Radar: A Review. *Remote Sensing* 2019; **11**. DOI:10.3390/rs11070879.

26 White CJ, Adnan MSG, Arosio M, *et al.* Review article: Towards multi-hazard and multi-risk indicators – a review and recommendations for development and implementation. 2024; published online Oct 8. DOI:10.5194/nhess-2024-178.

27 Sulfikkar Ahamed M, Sarmah T, Dabral A, Chatterjee R, Shaw R. Unpacking systemic, cascading, and compound risks: A case based analysis of Asia Pacific. *Progress in Disaster Science* 2023; **18**: 100285.

28 Woods D, McKeen T, Cunningham A, *et al.* Global gridded multi-temporal datasets to support human population distribution modelling. *Gates Open Res* 2025; **9**: 72.

29 Open Spatial Demographic Data and Research. WorldPop. https://www.worldpop.org/ (accessed Oct 13, 2025).

30 Home. Humanitarian OpenStreetMap Team. https://www.hotosm.org/ (accessed Oct 13, 2025).

31 Behling R, Roessner S, Kaufmann H, Kleinschmit B. Automated Spatiotemporal Landslide Mapping over Large Areas Using RapidEye Time Series Data. *Remote Sensing* 2014; **6**: 8026–55.

Preprint not peer reviewed

This preprint research paper has not been peer reviewed. Electronic copy available at: https://ssrn.com/abstract=7353571

32 Mondini AC, Guzzetti F, Reichenbach P, Rossi M, Cardinali M, Ardizzone F. Semi-automatic recognition and mapping of rainfall induced shallow landslides using optical satellite images. *Remote Sensing of Environment* 2011; **115**. DOI:10.1016/j.rse.2011.03.006.

33 Alfieri L, Burek P, Dutra E, Krzeminski B, Muraro D, Thielen J, Pappenberger F. GloFAS – global ensemble streamflow forecasting and flood early warning. Hydrology and Earth System Sciences 2013; 17: 1161–75.

34 Funk C, Peterson P, Harrison L, et al. The Climate Hazards Center Infrared Precipitation with Stations, Version 3. Scientific Data 2026; 13: 718. DOI:10.1038/s41597-026-07096-4.

35 Beck HE, Wood EF, Pan M, Fisher CK, Miralles DG, van Dijk AIJM, McVicar TR, Adler RF. MSWEP V2 global 3-hourly 0.1° precipitation: methodology and quantitative assessment. Bulletin of the American Meteorological Society 2019; 100: 473–500.

36 Amante C, Eakins BW. ETOPO1 1 arc-minute global relief model: procedures, data sources and analysis. NOAA Technical Memorandum NESDIS NGDC-24. Boulder, CO: National Geophysical Data Center, NOAA, 2009. DOI:10.7289/V5C8276M.

37 Cohen S, Raney A, Munasinghe D, et al. The Floodwater Depth Estimation Tool (FwDET v2.0) for improved remote sensing analysis of coastal flooding. Natural Hazards and Earth System Sciences 2019; 19: 2053–65.

Results – Figures and Tables

Spatial Distribution of JJASO (June-Oct / Oct-Nov) Flood Events across South Asia (2025)

Preprint not peer reviewed

This preprint research paper has not been peer reviewed. Electronic copy available at: https://ssrn.com/abstract=7353571

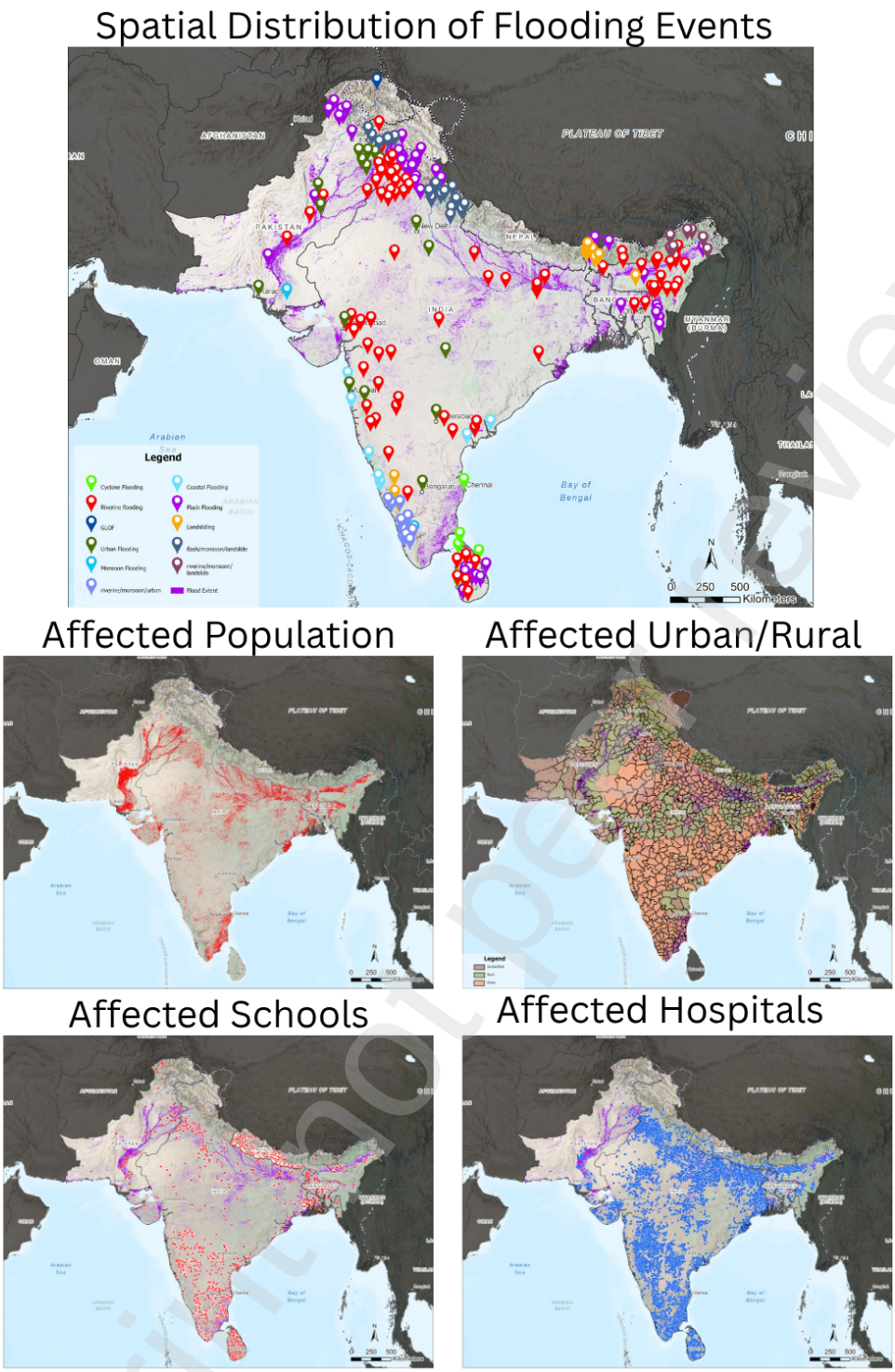


Figure 1. Spatial distribution and impacts of flood hazards across South Asia

Top panel shows the geographic distribution of recorded flood events, categorized by flood type (e.g., riverine, urban, flash, coastal, and landslide-related). Bottom panels illustrate the spatial extent of impacts: (left) affected population density, (middle) distribution of affected urban and rural areas, (bottom left) locations of exposed schools, and (bottom right) affected hospitals. Together, the maps highlight the concentration of flood exposure along major river basins, coastal regions, and densely populated areas.

This preprint research paper has not been peer reviewed. Electronic copy available at: https://ssrn.com/abstract=7353571

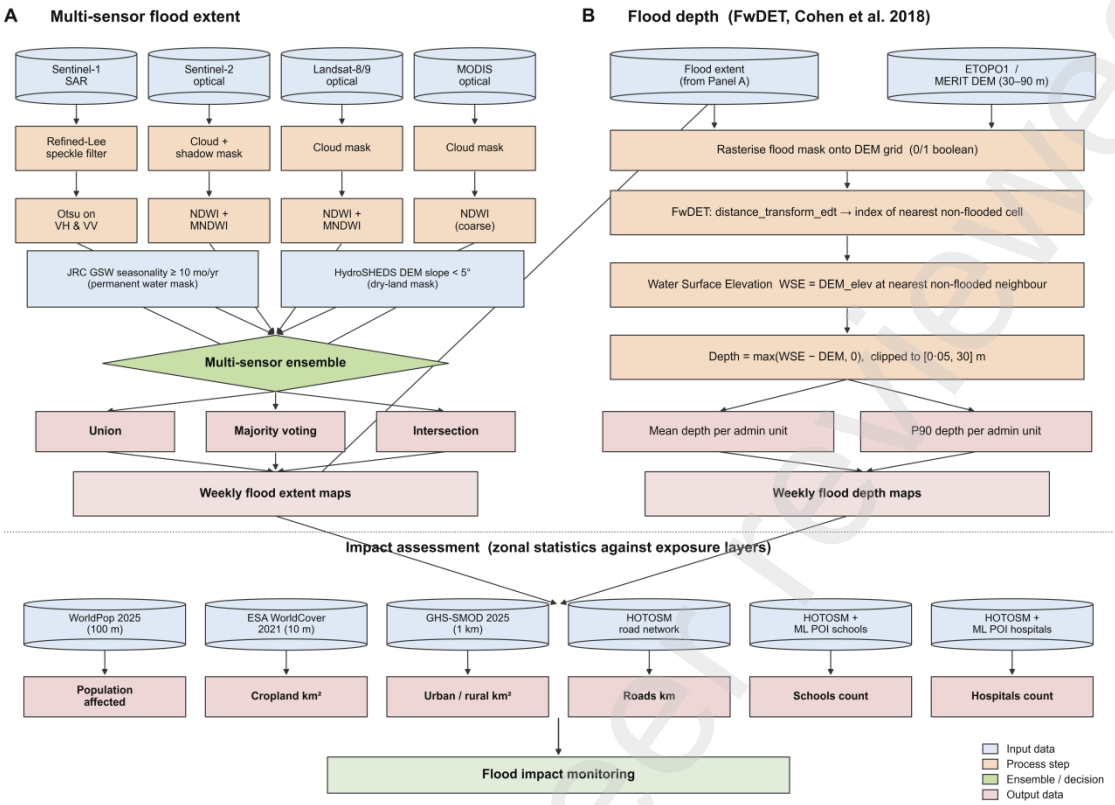


Figure 2. Flood inundation, depth, and impact assessment framework

(A) Multi-sensor flood extent from Sentinel-1 SAR and Sentinel-2, Landsat-8/9, and MODIS optical imagery, with JRC Global Surface Water and HydroSHEDS slope masks removing permanent water and steep terrain; a per-pixel ensemble yields Union and Intersection extent products. (B) Flood depth derived with the Floodwater Depth Estimation Tool (FwDET; Cohen et al 2018) from the Panel A extent and a digital elevation model, reporting mean and 90th-percentile depth per administrative unit. Zonal statistics against WorldPop, ESA WorldCover, GHS-SMOD, HOTOSM roads, and HOTOSM + machine-learning schools and hospitals yield the impact metrics used for flood impact monitoring.

Preprint not peer reviewed

This preprint research paper has not been peer reviewed. Electronic copy available at: https://ssrn.com/abstract=7353571

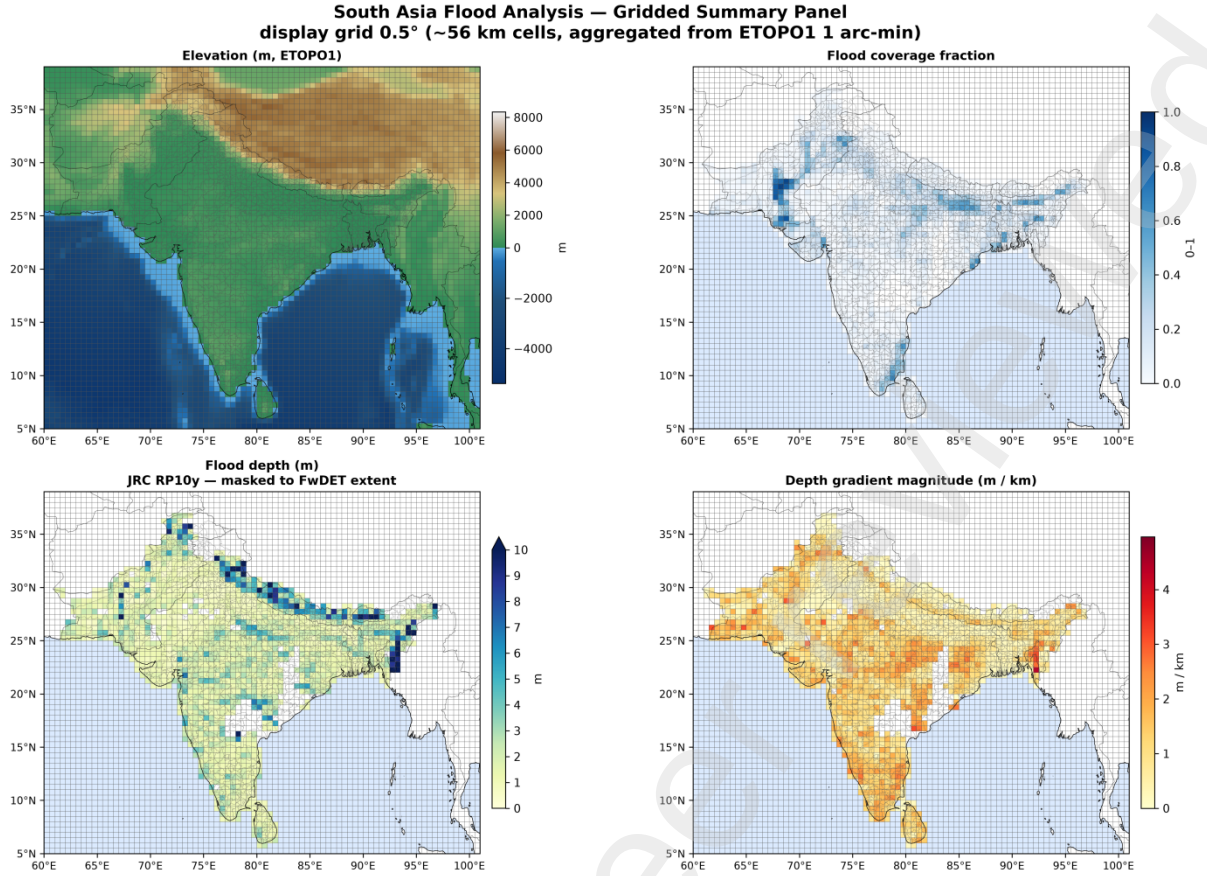


Figure 3. Gridded (0.5°, ~56 km) summary of the depth pipeline over South Asia

(a) ETOPO1 elevation, (b) observed flood coverage fraction, (c) JRC RP10y flood depth masked to the FwDET-derived flood footprint, and (d) depth-gradient magnitude. Panel (c) is the depth field used for all >1.5 m and >2 m exposure statistics.

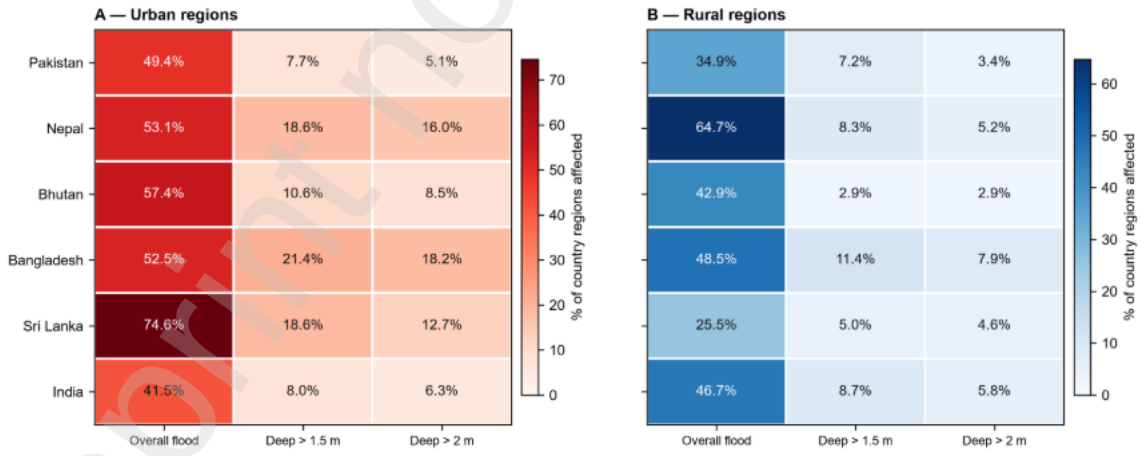


Figure 4. Percentage of each country's urban and rural regions affected (GHS-SMOD 2025 connected components)

This preprint research paper has not been peer reviewed. Electronic copy available at: https://ssrn.com/abstract=7353571

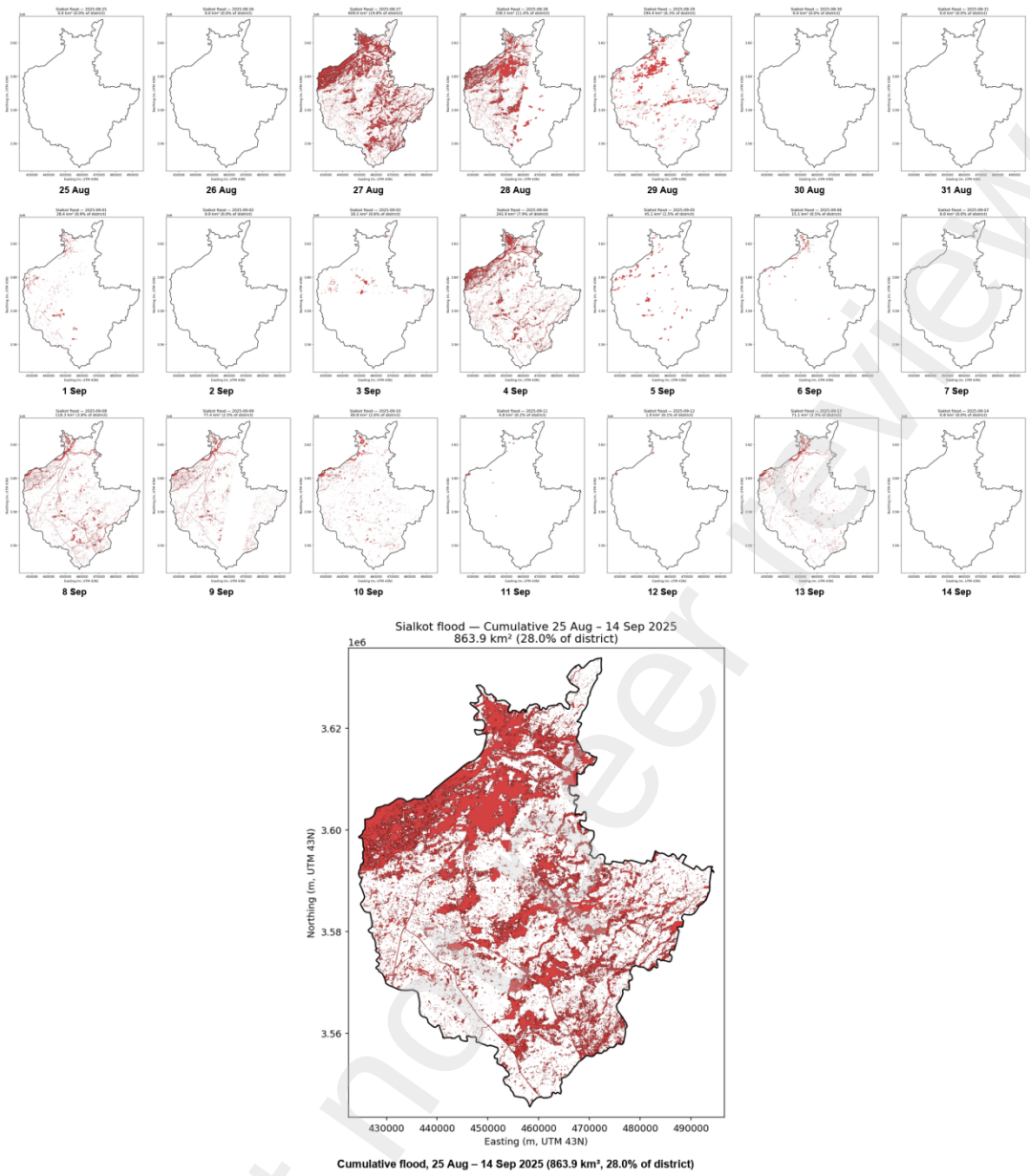


Figure 5. Operational daily nowcasting of composite flash and riverine flood in Sialkot district using a fusion of five satellite sensors.

HLS Sentinel-2, Sentinel-1 SAR, HLS Landsat-30, VIIRS, and MODIS. Each daily panel (25 August–14 September 2025) depicts the inundation footprint derived from the logical union of water detections across all sensors that acquired imagery over Sialkot on the corresponding date. The bottom panel presents the cumulative flood extent, obtained by combining all 21 daily masks (863.9 km², 28.0% of the district), which closely agrees with an independent cumulative reference product. The complementary revisit intervals and spectral capabilities of the five sensors mitigate observational gaps arising from cloud cover and limited single-sensor coverage, demonstrating that the proposed multi-sensor fusion framework enables near-real-

This preprint research paper has not been peer reviewed. Electronic copy available at: https://ssrn.com/abstract=7353571

time, daily-resolution flood nowcasting throughout a multi-week event.

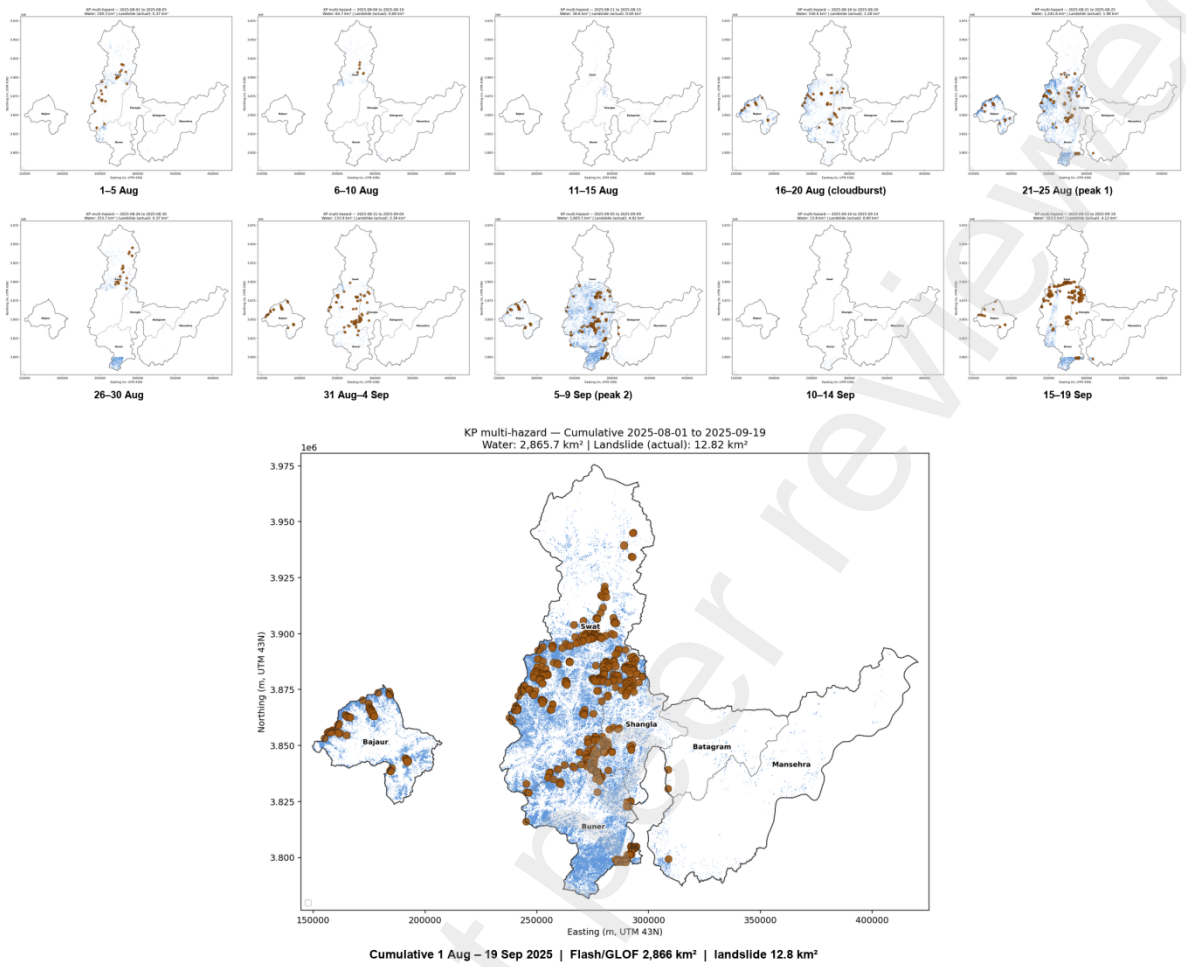


Figure 6. Daily multi-hazard nowcasting in mountainous Khyber-Pakhtunkhwa during the August–September 2025 monsoon,

illustrated across six districts: Buner, Bajaur, Swat, Shangla, Mansehra, and Batagram (~15,400 km² in total). Each panel presents the hazard footprint for a 5-day epoch generated by the multi-sensor fusion framework. Rapid-onset flood hazard (blue), encompassing flash floods and glacial-lake-outburst flows, is identified through bi-temporal change detection across HLS Sentinel-2, Sentinel-1 SAR, HLS Landsat-30, VIIRS, and MODIS, requiring concordance from at least two of the five sensors; no slope eligibility filter is imposed, given that mountain water itself is the detection target. Landslide hazard (brown) is delineated from co-registered HLS L30 and S30 imagery using a threshold rule based on NDVI and NBR loss ($\Delta NDVI < -0.15$; $\Delta NBR < -0.10$; post-event $NDVI < 0.40$), restricted to slopes ≥ 15°, in accordance with Behling et al. (2014)[31] and Mondini et al. (2011).[32] The temporal sequence resolves two distinct hazard pulses: a cloudburst on 16–25 August (peak 1; 1,241 km² of inundation across Buner, Shangla, and Mansehra), followed by a second monsoon surge on 5–9 September (peak 2; 1,604 km²). Landslide detections accumulate after the flood pulses, with peaks at epochs 7–8 and 10, reflecting the

This preprint research paper has not been peer reviewed. Electronic copy available at: https://ssrn.com/abstract=7353571

delayed mass-wasting that follows saturation of steep slopes. The final panel aggregates all 10 epochs (cumulative inundation: 2,866 km², ~18.6% of the region; cumulative landslide area: 12.8 km², ~0.08%). These findings demonstrate that the same five-satellite fusion framework deployed for nationwide riverine flood monitoring in Pakistan extends naturally to flash floods, GLOFs, and landslides in mountainous terrain, providing operational nowcasting capability across the full spectrum of hydro-meteorological hazards triggered by the 2025 monsoon.

2026 Live Flood Impact Monitoring Dashboard

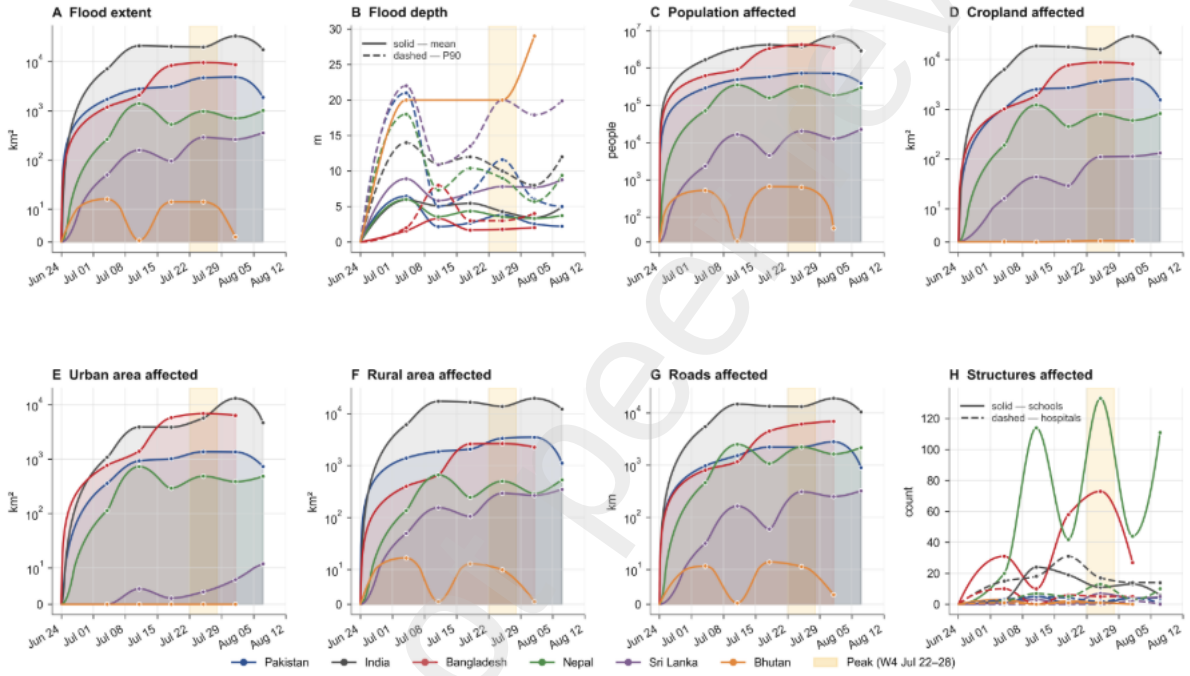
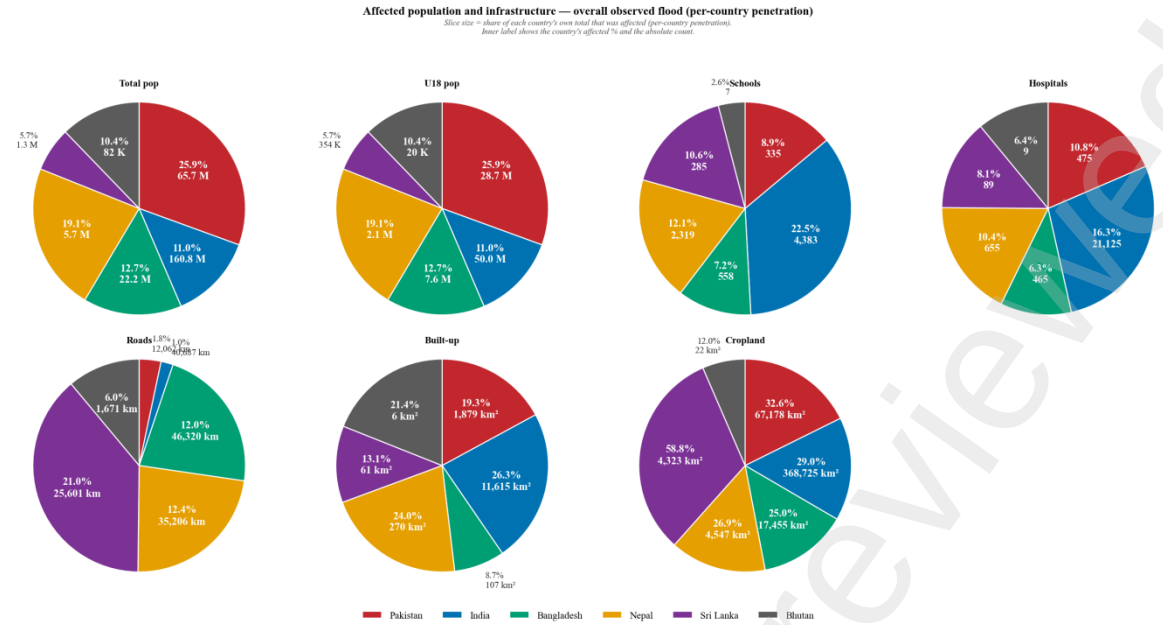


Figure 7. Weekly 2026 flood impact monitoring across six South Asian countries, 1 July – 8 August 2026.

Panels A–H show weekly flood extent (A), depth (B), affected population (C), cropland (D), urban area (E), rural area (F), roads (G), and schools/hospitals (H). Values before 1 July shown at zero to indicate the continuous monitoring baseline. The peak week (Jul 22-28) is shaded in amber. Panels A, C-G use a symmetric log scale; panels B and H use linear scale.

This preprint research paper has not been peer reviewed. Electronic copy available at: https://ssrn.com/abstract=7353571



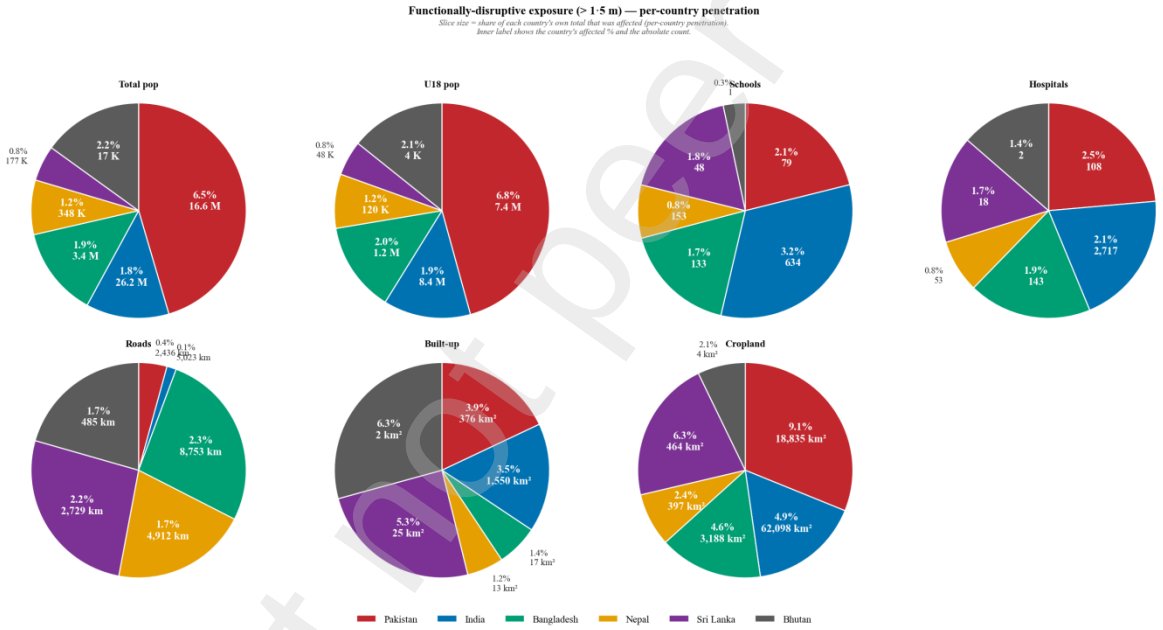


Figure 8. Country-normalized exposure — overall observed flood and deep water (JRC RP10y > 1·5 m).

Seven-metric panel showing, for each country, the share of that country's national total that was flood-affected. Slice size equals the country's penetration (affected ÷ country total) for the metric. Inner labels show the country's percentage and the absolute affected count. Slice angles compare countries within the same metric; the six per-country percentages do not sum to 100%. Slice size again reflects each country's penetration of the metric at deep-water conditions.

Preprint not peer reviewed

This preprint research paper has not been peer reviewed. Electronic copy available at: https://ssrn.com/abstract=7353571

UNOSAT vs Delta Inundation Episode-Level Comparison – South Asia 2025

Country	Episode Time	UNOSAT Inundation Extent (km²)	Population Potentially Exposed (million)	Delta Episode Level Inundation Extent (km²)	Delta Continuous Monitoring Total JJASO (June-Oct / Nov-Dec) Inundation Extent (km²)	Difference (%)
Pakistan	26 Aug–7 Sep 2025	17,000	~5.9	16,838	114513.0 (13%)	97,750 (570%)
Sri Lanka	26–30 Nov 2025	3,600	0.27	3624	3624.0 (5%)	24 (0.6%)
Bangladesh	4–11 Jul, 22–29 Jul 2025	8,400 5,500	~7.7 ~5.1	8365 5539	20922.2 (14%)	7022 (50.5%)
Bhutan	N/A	N/A	N/A	N/A	714.8 (1.8%)	N/A
India	N/A	N/A	N/A	N/A	541342.6 (16%)	N/A
Nepal	N/A	N/A	N/A	N/A	8614.0 (5.8%)	N/A
Total		**34,500**			**689,000 (15%)**	

Table 1.
Comparison of inundation extent estimates from the proposed Delta approach and UNOSAT inundation maps across selected South Asia flood events (2025).
The table summarizes inundation extent (km²) derived from UNOSAT products and the corresponding estimates from the proposed Delta methodology for Pakistan, Sri Lanka, and Bangladesh. Results show strong agreement between the two approaches across multiple inundation episodes, demonstrating the reliability of the Delta-based framework for rapid inundation extent assessment. Associated UNOSAT product links are provided for reference.

Affected Total Population and Children Under 18:

Total Affected Population of South Asia	**257,665,858**
Total Affected Population U18 of South Asia	89,300,153

World Pop 2025					
Country	**Metric**	**Total Pop**	**U18 Pop**	**U18 Male Pop**	**U18 Female Pop**
Bangladesh	Total Pop	174,617,088	58,806,044	30,333,990	28,472,024
	Affected Pop	22,241,144	7,615,636	3,935,178	3,680,457
	%	**12.74%**	**12.95%**	**12.97%**	**12.95%**
Bhutan	Total Pop	793,943	203,253	105,322	97,931
	Affected Pop	82,429	20,021	10,375	9,646
	%	**10.38%**	**9.85%**	**9.85%**	**9.85%**
Nepal	Total Pop	29,628,168	9,940,200	5,097,640	4,842,562
	Affected Pop	5,664,088	2,090,930	1,078,468	1,012,462
	%	**19.12%**	**21.04%**	**21.16%**	**20.91%**

Preprint not peer reviewed

This preprint research paper has not been peer reviewed. Electronic copy available at: https://ssrn.com/abstract=7353571

Pakistan	Total Pop	253,203,200	108,965,624	55,706,524	53,258,924
	Affected Pop	65,714,056	28,652,836	14,639,274	14,013,576
	%	**25.95%**	**26.30%**	**26.28%**	**26.31%**
India	Total Pop	1,457,435,392	431,330,496	224,857,440	206,473,040
	Affected Pop	160,754,944	50,037,804	26,099,016	23,938,788
	%	**11.03%**	**11.60%**	**11.61%**	**11.59%**
Sri Lanka	Total Pop	23,162,792	6,150,290	3,130,547	3,019,738
	Affected Pop	3,209,197	882,926	449,321	433,604
	%	13.85%	14.36%	14.35%	14.36%
Total South Asia		257,665,858	89,300,153		

Table 2.

Estimated flood-affected population in South Asia (2025), including children under 18 by country and gender.

The table summarizes total and affected populations across South Asian countries, with a breakdown of children under 18 (U18), including male and female populations. Overall, approximately 257.7 million people are affected, of which 89.3 million are children. Country-level estimates highlight substantial impacts in India and Pakistan, both in absolute numbers and proportions, with children representing a significant share of the affected population. Percentage values indicate the proportion of affected individuals relative to national population totals.

Affected Cropland and Infrastructure – South Asia 2025

Country	Builtup Area (km^2)*	Cropland (km^2)*	Roads (km)†	Affected Schools (Count)†	Affected Hospitals (Count)†
Bangladesh	106.67 (8.69%)	17,455.30 (25.01%)	46,320.10 (12%)	558 (7.2%)	465 (6.3%)
Bhutan	6.00 (21.43%)	21.90 (11.99%)	1670.65 (6%)	7 (2.6%)	9 (6.4%)
India	11615.01 (26.33%)	368,724.85 (28.96%)	40687.02 (1%)	4383 (22.5%)	21125 (16.3%)
Nepal	269.85 (24%)	4,547.18 (26.95%)	35205.85 (12.4%)	2319 (12.1)	655 (10.4%)
Pakistan	1878.69 (19.29%)	67,177.80 (32.59%)	12062.05 (1.8%)	335 (8.9%)	475 (10.8%)
Sri Lanka	61.01 (13.14%)	4,322.98 (58.78%)	25,601.31 (21%)	285 (10.6%)	89 (8.1)
Total	13937.23 (25%)	462160.01 (29%)	75.52 thousand	7887 (14.9%)	22818 (15.3%)

Table 3.

Estimated flood impacts on cropland and critical infrastructure in South Asia (2025).

This table presents country-level estimates of affected built-up areas, cropland, road networks, schools, and hospitals, along with their respective proportions. Results show substantial impacts on agricultural land and infrastructure, with India and Pakistan

Preprint not peer reviewed

This preprint research paper has not been peer reviewed. Electronic copy available at: https://ssrn.com/abstract=7353571

contributing the largest absolute losses, while smaller countries exhibit higher relative impacts in specific sectors such as cropland and built-up areas.

Flood Extent (km²)			
Country	**Deep > 1.5 m**	**Deep > 2 m**	**SD (n=2)**
Pakistan	77,047.2 (8.75%)	39,581.3 (4.49%)	26,492.4
Nepal	6,558.0 (4.42%)	4,502.1 (3.03%)	1,453.8
Bhutan	582.9 (1.47%)	451.1 (1.14%)	93.25
Bangladesh	13,783.4 (9.22%)	6,644.6 (4.45%)	5,047.9
Sri Lanka	2,149.0 (2.96%)	674.0 (0.93%)	1,043.0
India	358,374.6 (10.59%)	175,406.5 (5.18%)	129,377.9
Total	458,495.1	227,259.6	163,508.2

Table 4.
Deep flood extent, built-up, cropland, roads

Population (million)			
Country	**Deep > 1.5 m**	**Deep > 2 m**	**SD (n=2)**
Pakistan	16,587,400 (6.55%)	8,872,790 (3.50%)	5,455,053
Nepal	348,084 (1.18%)	236,514 (0.80%)	78,892
Bhutan	17,198 (2.17%)	14,654 (1.85%)	1,798
Bangladesh	3,386,979 (1.94%)	1,957,772 (1.12%)	1,010,602
Sri Lanka	177,433 (0.77%)	138,255 (0.60%)	27,703
India	26,247,721 (1.80%)	17,323,001 (1.19%)	6,310,730
Total	46,764,815	28,542,986	12,884,779

Table 5.
Deep-water WorldPop Total (2025)

*ESA World Cover 2021 (https://developers.google.com/earth-engine/datasets/catalog/ESA_WorldCover_v200)

†Giga-HOTOSM: https://www.hotosm.org/en/

Preprint not peer reviewed

This preprint research paper has not been peer reviewed. Electronic copy available at: https://ssrn.com/abstract=7353571

Results – Main Text Figures and Tables

Improving health system resilience through continuous nowcasting of undetected public health disruption during floods: a multi-country precision intelligence study

Corresponding author: Professor Sara Khalid, University of Oxford, sara.khalid@ndorms.ox.ac.uk

on behalf of the Climate and Child Initiative Consortium

Preprint not peer reviewed

This preprint research paper has not been peer reviewed. Electronic copy available at: https://ssrn.com/abstract=7353571

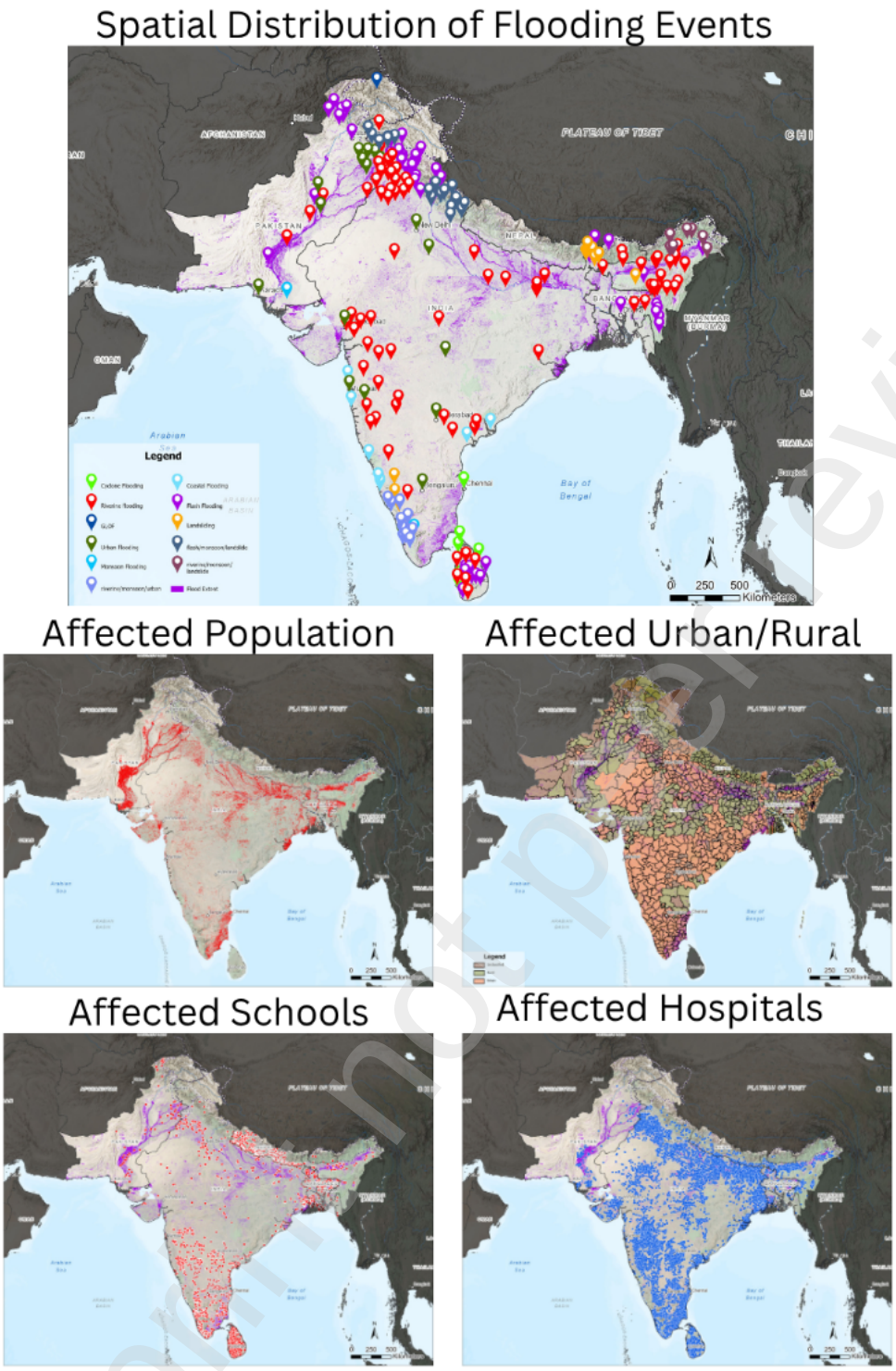


Figure 1. Spatial distribution and impacts of flood hazards across South Asia

Top panel shows the geographic distribution of recorded flood events, categorized by flood type (e.g., riverine, urban, flash, coastal, and landslide-related). Bottom panels illustrate the spatial extent of impacts: (left) affected population density, (middle) distribution of affected urban and rural areas, (bottom left) locations of exposed schools, and (bottom right) affected

Preprint not peer reviewed

This preprint research paper has not been peer reviewed. Electronic copy available at: https://ssrn.com/abstract=7353571

hospitals. Together, the maps highlight the concentration of flood exposure along major river basins, coastal regions, and densely populated areas.

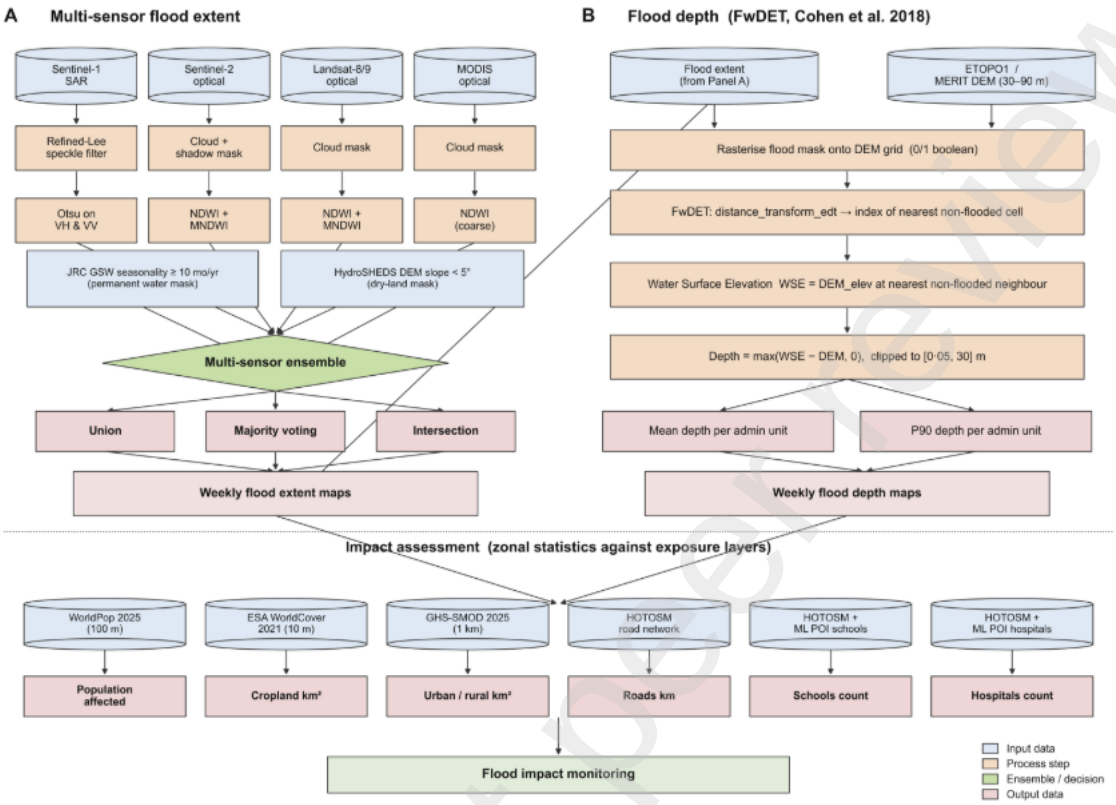


Figure 2. Flood inundation, depth, and impact assessment framework

(A) Multi-sensor flood extent from Sentinel-1 SAR and Sentinel-2, Landsat-8/9, and MODIS optical imagery, with JRC Global Surface Water and HydroSHEDS slope masks removing permanent water and steep terrain; a per-pixel ensemble yields Union and Intersection extent products. (B) Flood depth derived with the Floodwater Depth Estimation Tool (FwDET; Cohen et al 2018) from the Panel A extent and a digital elevation model, reporting mean and 90th-percentile depth per administrative unit. Zonal statistics against WorldPop, ESA WorldCover, GHS-SMOD, HOTOSM roads, and HOTOSM + machine-learning schools and hospitals yield the impact metrics used for flood impact monitoring.

Preprint not peer reviewed

This preprint research paper has not been peer reviewed. Electronic copy available at: https://ssrn.com/abstract=7353571

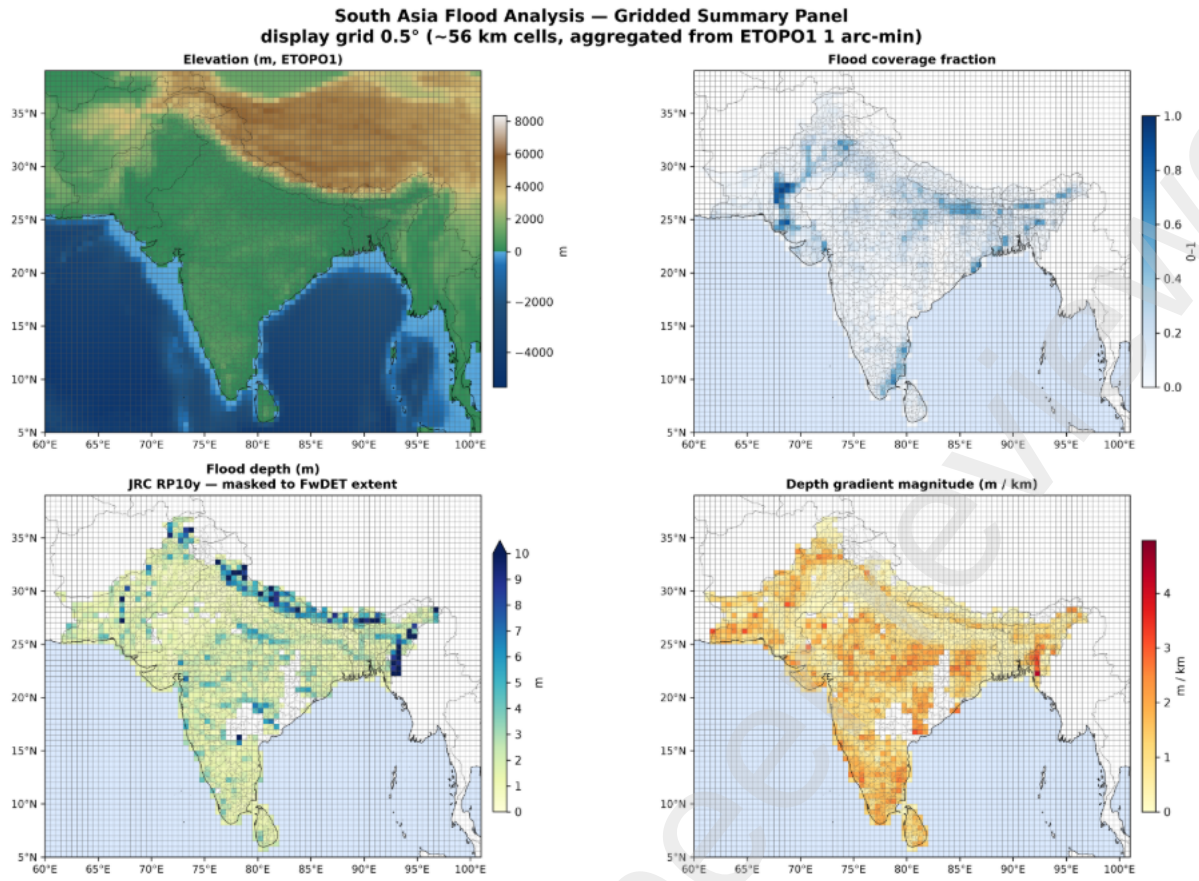


Figure 3. Gridded (0.5°, ~56 km) summary of the depth pipeline over South Asia

(a) ETOPO1 elevation, (b) observed flood coverage fraction, (c) JRC RP10y flood depth masked to the FwDET-derived flood footprint, and (d) depth-gradient magnitude. Panel (c) is the depth field used for all >1.5 m and >2 m exposure statistics.

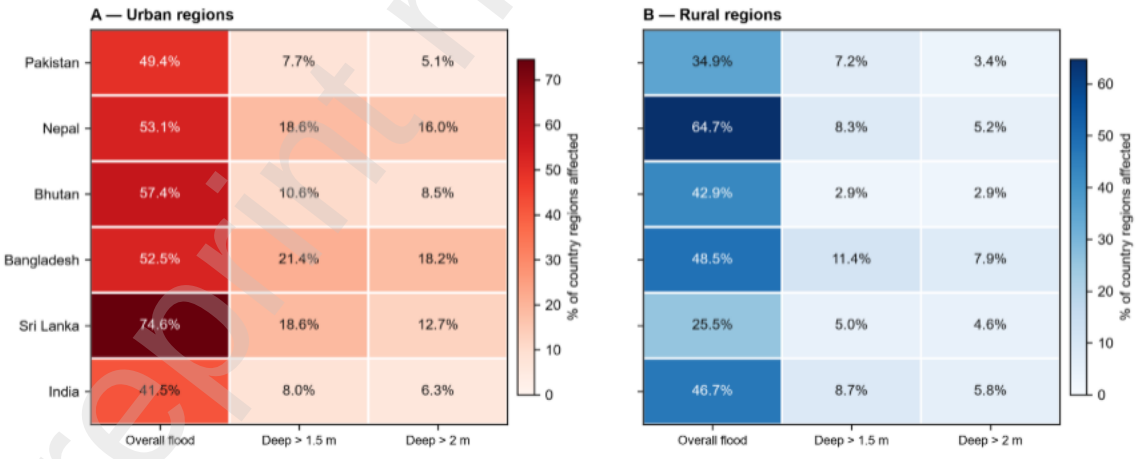


Figure 4. Percentage of each country's urban and rural regions affected (GHS-SMOD 2025 connected components)

Preprint not peer reviewed

This preprint research paper has not been peer reviewed. Electronic copy available at: https://ssrn.com/abstract=7353571

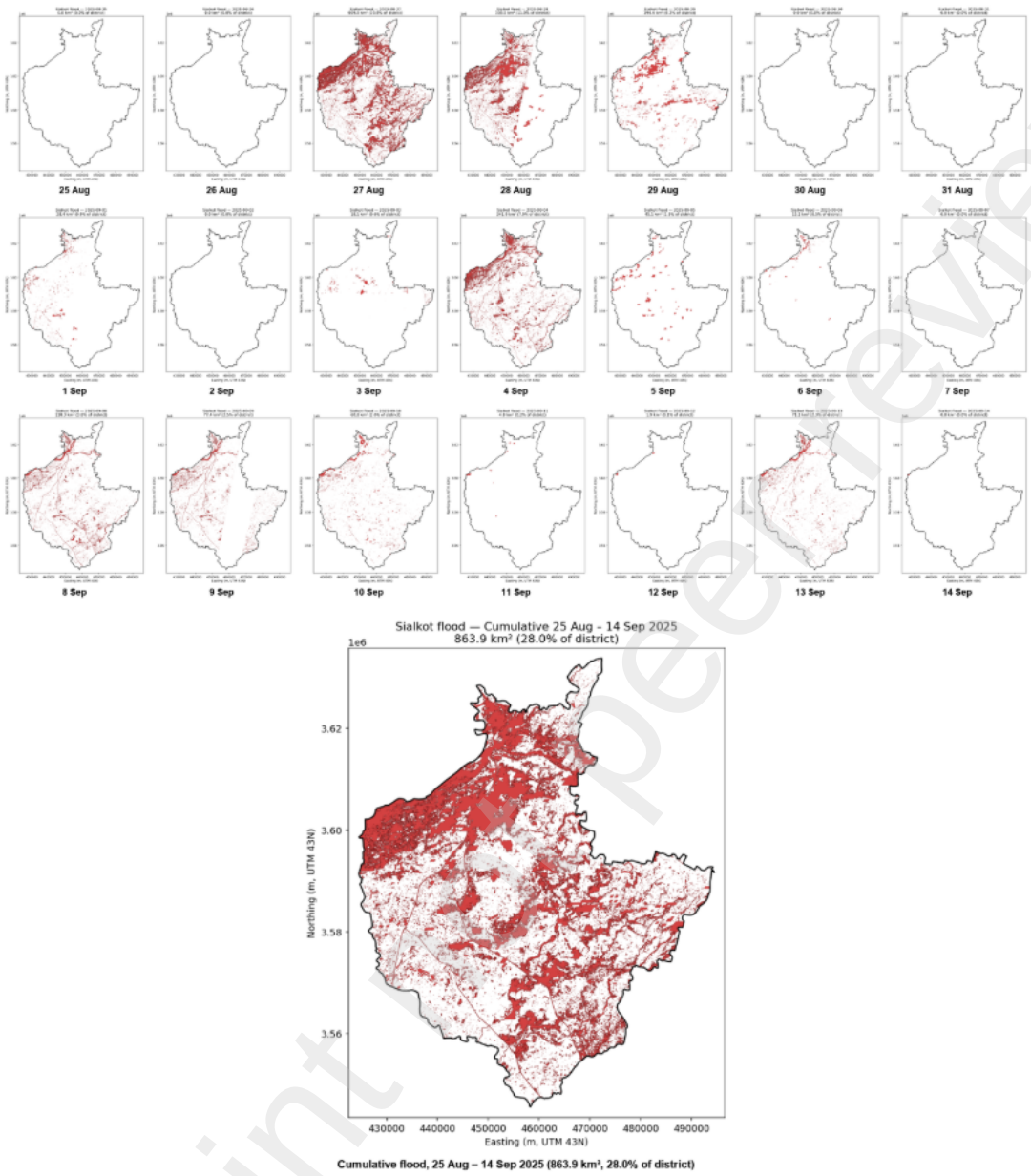


Figure 5. Operational daily nowcasting of composite flash and riverine flood in Sialkot district using a fusion of five satellite sensors.

HLS Sentinel-2, Sentinel-1 SAR, HLS Landsat-30, VIIRS, and MODIS. Each daily panel (25 August–14 September 2025) depicts the inundation footprint derived from the logical union of water detections across all sensors that acquired imagery over Sialkot on the corresponding date. The bottom panel presents the cumulative flood extent, obtained by combining all 21 daily masks (863.9 km², 28.0% of the district), which closely agrees with an independent cumulative reference product. The complementary revisit intervals and spectral capabilities of

Preprint not peer reviewed

This preprint research paper has not been peer reviewed. Electronic copy available at: https://ssrn.com/abstract=7353571

the five sensors mitigate observational gaps arising from cloud cover and limited single-sensor coverage, demonstrating that the proposed multi-sensor fusion framework enables near-real-time, daily-resolution flood nowcasting throughout a multi-week event.

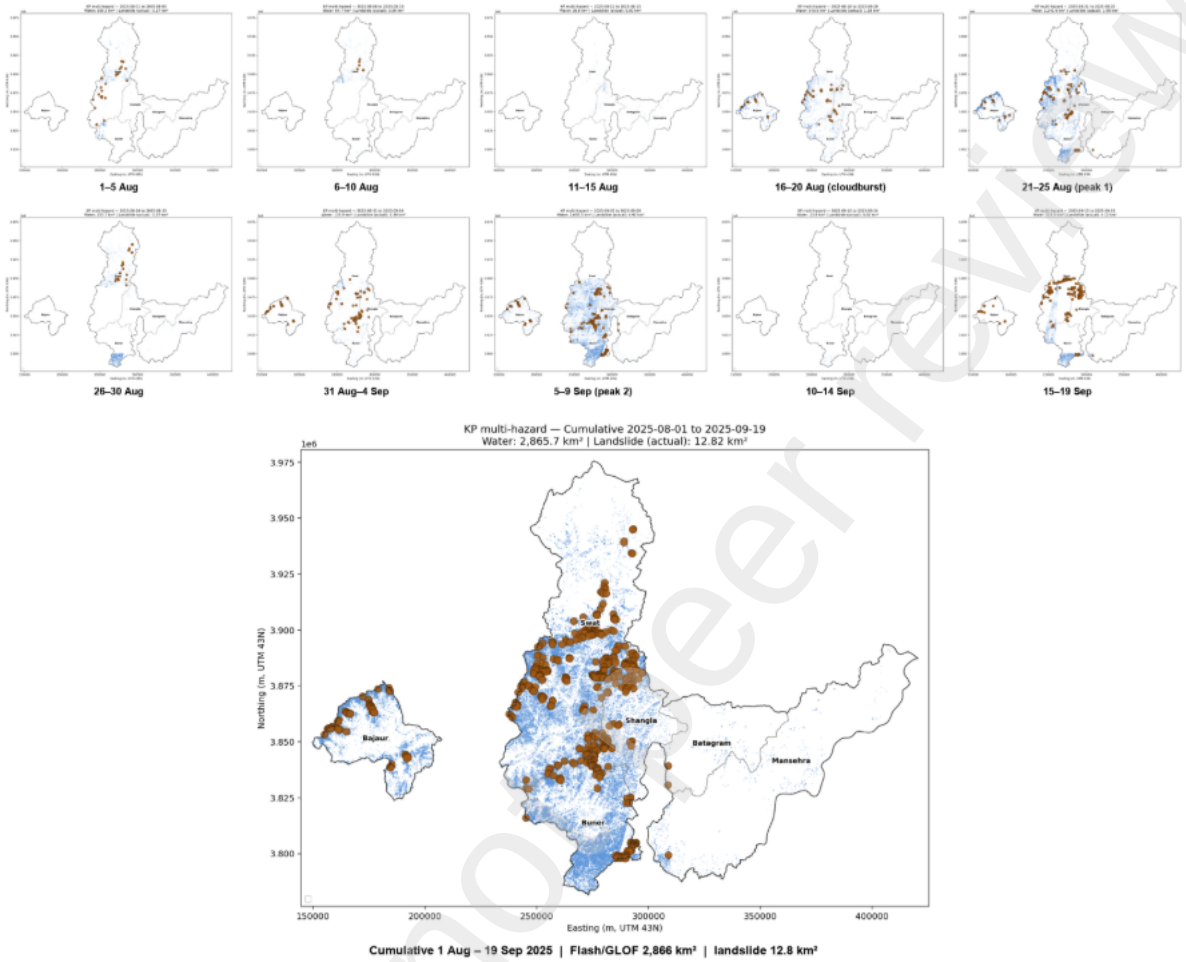


Figure 6. Daily multi-hazard nowcasting in mountainous Khyber-Pakhtunkhwa during the August–September 2025 monsoon,

illustrated across six districts: Buner, Bajaur, Swat, Shangla, Mansehra, and Batagram (~15,400 km² in total). Each panel presents the hazard footprint for a 5-day epoch generated by the multi-sensor fusion framework. Rapid-onset flood hazard (blue), encompassing flash floods and glacial-lake-outburst flows, is identified through bi-temporal change detection across HLS Sentinel-2, Sentinel-1 SAR, HLS Landsat-30, VIIRS, and MODIS, requiring concordance from at least two of the five sensors; no slope eligibility filter is imposed, given that mountain water itself is the detection target. Landslide hazard (brown) is delineated from co-registered HLS L30 and S30 imagery using a threshold rule based on NDVI and NBR loss ($\Delta NDVI < -0.15$; $\Delta NBR < -0.10$; post-event $NDVI < 0.40$), restricted to slopes ≥ 15°, in accordance with Behling et al. (2014)[31] and Mondini et al. (2011).[32] The temporal sequence resolves two distinct hazard pulses: a cloudburst on 16–25 August (peak 1; 1,241 km² of

Preprint not peer reviewed

This preprint research paper has not been peer reviewed. Electronic copy available at: https://ssrn.com/abstract=7353571

inundation across Buner, Shangla, and Mansehra), followed by a second monsoon surge on 5–9 September (peak 2; 1,604 km²). Landslide detections accumulate after the flood pulses, with peaks at epochs 7–8 and 10, reflecting the delayed mass-wasting that follows saturation of steep slopes. The final panel aggregates all 10 epochs (cumulative inundation: 2,866 km², ~18.6% of the region; cumulative landslide area: 12.8 km², ~0.08%). These findings demonstrate that the same five-satellite fusion framework deployed for nationwide riverine flood monitoring in Pakistan extends naturally to flash floods, GLOFs, and landslides in mountainous terrain, providing operational nowcasting capability across the full spectrum of hydro-meteorological hazards triggered by the 2025 monsoon.

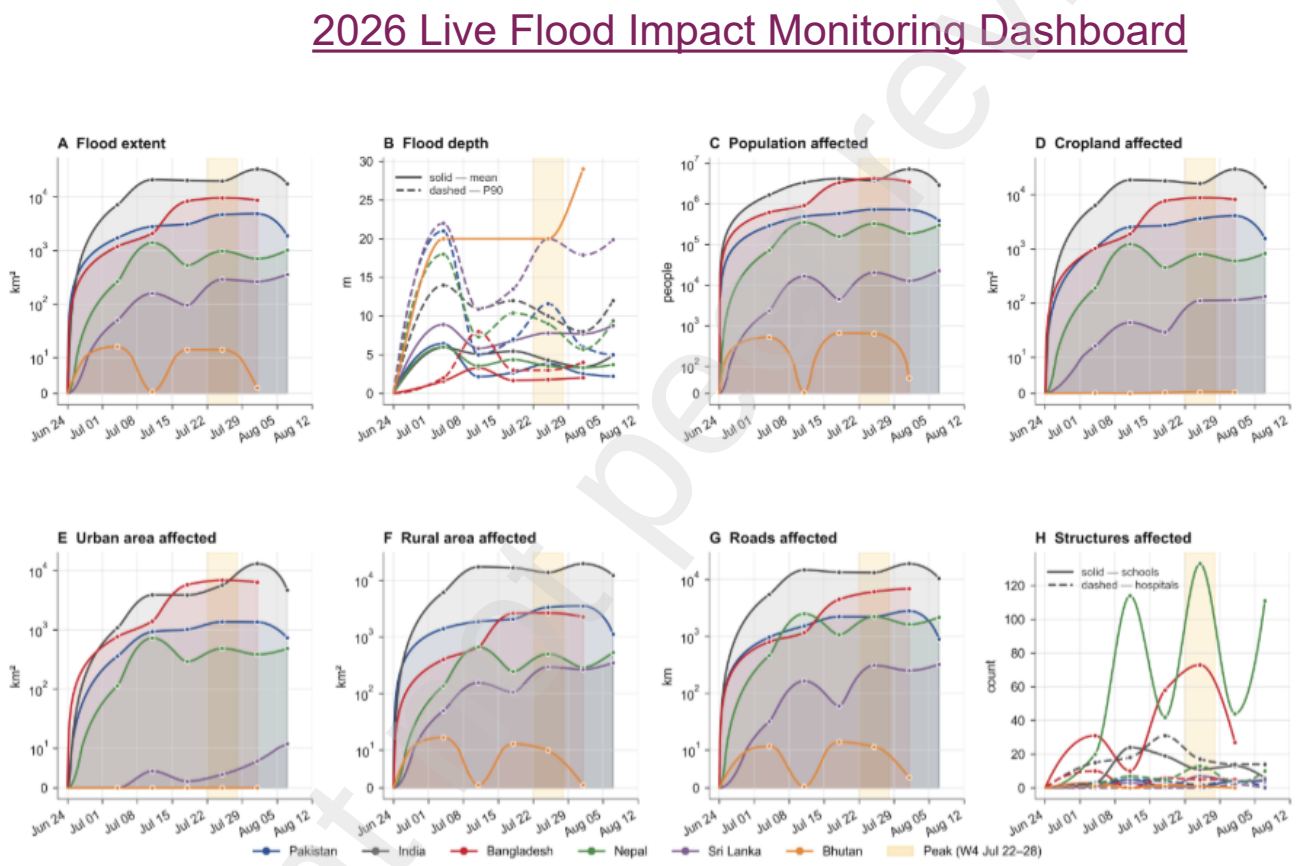


Figure 7. Weekly 2026 flood impact monitoring across six South Asian countries, 1 July – 8 August 2026.

Panels A–H show weekly flood extent (A), depth (B), affected population (C), cropland (D), urban area (E), rural area (F), roads (G), and schools/hospitals (H). Values before 1 July shown at zero to indicate the continuous monitoring baseline. The peak week (Jul 22-28) is shaded in amber. Panels A, C-G use a symmetric log scale; panels B and H use linear scale.

Preprint not peer reviewed

This preprint research paper has not been peer reviewed. Electronic copy available at: https://ssrn.com/abstract=7353571

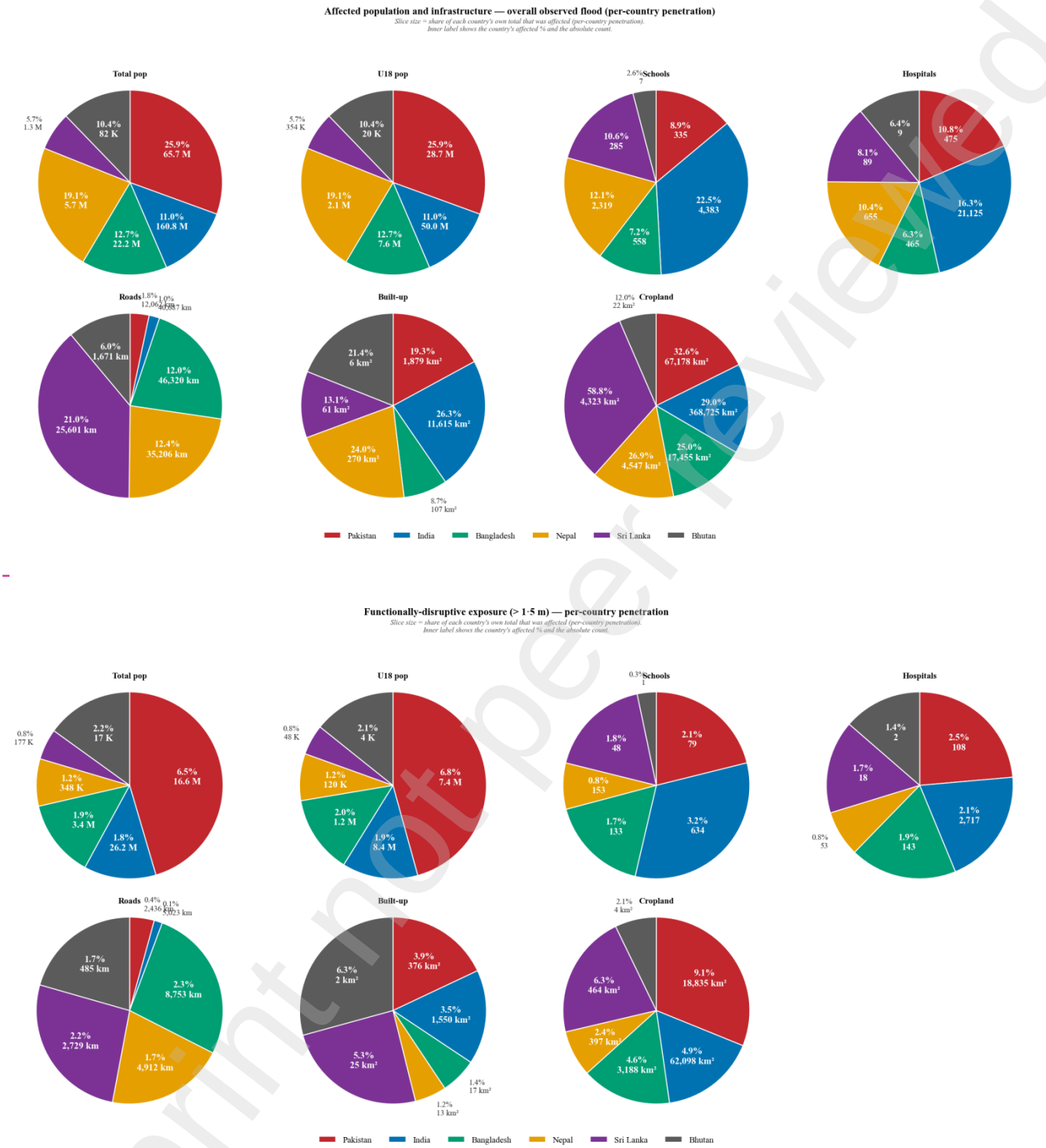


Figure 8. Country-normalized exposure — overall observed flood and deep water (JRC RP10y > 1·5 m).

Seven-metric panel showing, for each country, the share of that country's national total that was flood-affected. Slice size equals the country's penetration (affected ÷ country total) for the metric. Inner labels show the country's percentage and the absolute affected count. Slice angles compare countries within the same metric; the six per-country percentages do not sum

Preprint not peer reviewed

This preprint research paper has not been peer reviewed. Electronic copy available at: https://ssrn.com/abstract=7353571

to 100%. Slice size again reflects each country's penetration of the metric at deep-water conditions.

UNOSAT vs Delta Inundation Episode-Level Comparison – South Asia 2025

Country	Episode Time	UNOSAT Inundation Extent (km²)	Population Potentially Exposed (million)	Delta Episode Level Inundation Extent (km²)	Delta Continuous Monitoring Total JJASO (June-Oct / Nov-Dec) Inundation Extent (km²)	Difference (%)
Pakistan	26 Aug–7 Sep 2025	17,000	~5.9	16,838	114513.0 (13%)	97,750 (570%)
Sri Lanka	26–30 Nov 2025	3,600	0.27	3624	3624.0 (5%)	24 (0.6%)
Bangladesh	4–11 Jul, 22–29 Jul 2025	8,400 5,500	~7.7 ~5.1	8365 5539	20922.2 (14%)	7022 (50.5%)
Bhutan	N/A	N/A	N/A	N/A	714.8 (1.8%)	N/A
India	N/A	N/A	N/A	N/A	541342.6 (16%)	N/A
Nepal	N/A	N/A	N/A	N/A	8614.0 (5.8%)	N/A
Total		**34,500**			**689,000 (15%)**	

Table 1.
Comparison of inundation extent estimates from the proposed Delta approach and UNOSAT inundation maps across selected South Asia flood events (2025).
The table summarizes inundation extent (km²) derived from UNOSAT products and the corresponding estimates from the proposed Delta methodology for Pakistan, Sri Lanka, and Bangladesh. Results show strong agreement between the two approaches across multiple inundation episodes, demonstrating the reliability of the Delta-based framework for rapid inundation extent assessment. Associated UNOSAT product links are provided for reference.

Affected Total Population and Children Under 18:

Total Affected Population of South Asia	**257,665,858**
Total Affected Population U18 of South Asia	89,300,153

World Pop 2025					
Country	**Metric**	**Total Pop**	**U18 Pop**	**U18 Male Pop**	**U18 Female Pop**
Bangladesh	Total Pop	174,617,088	58,806,044	30,333,990	28,472,024
	Affected Pop	22,241,144	7,615,636	3,935,178	3,680,457
	%	**12.74%**	**12.95%**	**12.97%**	**12.95%**
Bhutan	Total Pop	793,943	203,253	105,322	97,931
	Affected Pop	82,429	20,021	10,375	9,646

Preprint not peer reviewed

This preprint research paper has not been peer reviewed. Electronic copy available at: https://ssrn.com/abstract=7353571

	%	**10.38%**	**9.85%**	**9.85%**	**9.85%**
Nepal	Total Pop	29,628,168	9,940,200	5,097,640	4,842,562
	Affected Pop	5,664,088	2,090,930	1,078,468	1,012,462
	%	**19.12%**	**21.04%**	**21.16%**	**20.91%**
Pakistan	Total Pop	253,203,200	108,965,624	55,706,524	53,258,924
	Affected Pop	65,714,056	28,652,836	14,639,274	14,013,576
	%	**25.95%**	**26.30%**	**26.28%**	**26.31%**
India	Total Pop	1,457,435,392	431,330,496	224,857,440	206,473,040
	Affected Pop	160,754,944	50,037,804	26,099,016	23,938,788
	%	**11.03%**	**11.60%**	**11.61%**	**11.59%**
Sri Lanka	Total Pop	23,162,792	6,150,290	3,130,547	3,019,738
	Affected Pop	3,209,197	882,926	449,321	433,604
	%	13.85%	14.36%	14.35%	14.36%
Total South Asia		257,665,858	89,300,153		

Table 2.

Estimated flood-affected population in South Asia (2025), including children under 18 by country and gender.

The table summarizes total and affected populations across South Asian countries, with a breakdown of children under 18 (U18), including male and female populations. Overall, approximately 257.7 million people are affected, of which 89.3 million are children. Country-level estimates highlight substantial impacts in India and Pakistan, both in absolute numbers and proportions, with children representing a significant share of the affected population. Percentage values indicate the proportion of affected individuals relative to national population totals.

Affected Cropland and Infrastructure – South Asia 2025

Country	Builtup Area (km^2)*	Cropland (km^2)*	Roads (km)†	Affected Schools (Count)†	Affected Hospitals (Count)†
Bangladesh	106.67 (8.69%)	17,455.30 (25.01%)	46,320.10 (12%)	558 (7.2%)	465 (6.3%)
Bhutan	6.00 (21.43%)	21.90 (11.99%)	1670.65 (6%)	7 (2.6%)	9 (6.4%)
India	11615.01 (26.33%)	368,724.85 (28.96%)	40687.02 (1%)	4383 (22.5%)	21125 (16.3%)
Nepal	269.85 (24%)	4,547.18 (26.95%)	35205.85 (12.4%)	2319 (12.1)	655 (10.4%)
Pakistan	1878.69 (19.29%)	67,177.80 (32.59%)	12062.05 (1.8%)	335 (8.9%)	475 (10.8%)
Sri Lanka	61.01 (13.14%)	4,322.98 (58.78%)	25,601.31 (21%)	285 (10.6%)	89 (8.1)
Total	13937.23 (25%)	462160.01 (29%)	75.52 thousand	7887 (14.9%)	22818 (15.3%)

Preprint not peer reviewed

This preprint research paper has not been peer reviewed. Electronic copy available at: https://ssrn.com/abstract=7353571

Table 3.

Estimated flood impacts on cropland and critical infrastructure in South Asia (2025).
This table presents country-level estimates of affected built-up areas, cropland, road networks, schools, and hospitals, along with their respective proportions. Results show substantial impacts on agricultural land and infrastructure, with India and Pakistan contributing the largest absolute losses, while smaller countries exhibit higher relative impacts in specific sectors such as cropland and built-up areas.

Flood Extent (km²)			
Country	**Deep > 1.5 m**	**Deep > 2 m**	**SD (n=2)**
Pakistan	77,047.2 (8.75%)	39,581.3 (4.49%)	26,492.4
Nepal	6,558.0 (4.42%)	4,502.1 (3.03%)	1,453.8
Bhutan	582.9 (1.47%)	451.1 (1.14%)	93.25
Bangladesh	13,783.4 (9.22%)	6,644.6 (4.45%)	5,047.9
Sri Lanka	2,149.0 (2.96%)	674.0 (0.93%)	1,043.0
India	358,374.6 (10.59%)	175,406.5 (5.18%)	129,377.9
Total	458,495.1	227,259.6	163,508.2

Table 4.

Deep flood extent, built-up, cropland, roads

Population (million)			
Country	**Deep > 1.5 m**	**Deep > 2 m**	**SD (n=2)**
Pakistan	16,587,400 (6.55%)	8,872,790 (3.50%)	5,455,053
Nepal	348,084 (1.18%)	236,514 (0.80%)	78,892
Bhutan	17,198 (2.17%)	14,654 (1.85%)	1,798
Bangladesh	3,386,979 (1.94%)	1,957,772 (1.12%)	1,010,602
Sri Lanka	177,433 (0.77%)	138,255 (0.60%)	27,703
India	26,247,721 (1.80%)	17,323,001 (1.19%)	6,310,730
Total	46,764,815	28,542,986	12,884,779

Table 5.

Deep-water WorldPop Total (2025)

*ESA World Cover 2021 (https://developers.google.com/earth-engine/datasets/catalog/ESA_WorldCover_v200)

†Giga-HOTOSM: https://www.hotosm.org/en/

Preprint not peer reviewed

This preprint research paper has not been peer reviewed. Electronic copy available at: https://ssrn.com/abstract=7353571